AN ABSTRACT OF THE THESIS OF

Sasirekha Kodialam for the degree of Doctor of Philosophy in Chemistry presented on July 25, 1994.

Title: Complex Oxides of 6p Block Elements

Redacted for Privacy

Abstract approved: _____
A. W. Sleight

This work involves the synthesis and characterization of oxides of 6p block elements. The possibility of using synthesis methods like electrodeposition and low temperature hydrothermal methods has been explored. New phases were obtained in the low temperature hydrothermal method, and single crystals of a known compound were obtained for the first time by electrodeposition. These compounds were structurally characterized by diffraction methods - X-ray powder and single crystal diffraction. Structural aspects of $KBiO_3$ and related compounds were studied in greater detail due to the availability of single crystals. The reasons for variation in lattice parameter were attributed to the presence of water of hydration and due to the presence of Bi^{3+} in the potassium site. Mixed valent bismuth cadmium oxide was synthesized for the first time using hydrothermal synthesis. A new structure type with a unique structure, $HBi_3(CrO_4)_2O_3$, was also synthesized by hydrothermal synthesis. The location of protons in the structure was predicted using the bond valence approach.

In addition to the exploration of new synthesis techniques, oxides prepared by conventional solid-state synthesis have been studied systematically. The structures of oxides in the $Tl_2Nb_2O_{6+x}$ system with change in oxidation state of thallium have been refined using neutron diffraction data. The refinements gave accurate information about the oxygen content, non-stoichiometry in the thallium site, mixing of Tl^{III} in the niobium site and the thermal parameter for compounds in the system with different oxygen content.

Complex Oxides of 6p Block Elements

by

Sasirekha Kodialam

A THESIS

submitted to

Oregon State University

in partial fulfillment of
the requirements for the
degree of

Doctor of Philosophy

Completed July 25, 1994

Commencement June 1995

APPROVED:

Redacted for Privacy

Professor of Chemistry in charge of major

Redacted for Privacy

Head of department of Chemistry

Redacted for Privacy

Dean of Graduate School

Date thesis is presented July 25, 1994

Typed by researcher for Sasirekha Kodialam

To

My Parents and Sisters

Acknowledgments

I would like to thank my advisor, Dr. A.W. Sleight for his guidance throughout the course of my research. He has introduced me to a variety of aspects of solid state chemistry. Being a part of his research group was a good learning experience.

Members of my committee, Drs. D. Keszler, M. Lerner, J. Ingle and P.S. Ho have offered useful suggestions in my thesis.

My interaction with the other graduate students in the lab, Vincent Korthuis, Phong Nguyen, Pat Woodward, Nazy Khosrovani, Paul Bacon and Matt Hall has helped me in better understanding various research tools. I am thankful to them for making my research atmosphere very pleasant.

I would like to thank Dr. Nobuhiro Kumada of Yamanashi University, Japan with whom I had an opportunity to interact with when he was a visiting professor in our group.

I have also enjoyed the discussions with the postdocs in our group, Dr. Rolf Hoffmann, Dr. Laura King, Dr. Ruiping Wang, Dr. Richard Mackay, Dr. Jianguo Hou, Dr. Mary Thundathil.

I enjoyed the friendship and discussions I had with Annapoorna Akella. She also helped me to get started with the single crystal work.

I thank Ms. Cheryl A. Hills for her assistance with manuscript preparation.

I thank Dr. M.A. Subramanian of Dupont for providing us with the high pressure sample of thallium niobium oxide.

My family in India has been extremely supportive and encouraging throughout my school years. My mother, Mrs. K.Vasantha, and father, Mr. K. Raman, have always been a positive influence on me. My sisters in

India, Radhika and Latha have supported me in pursuing this doctoral degree. I would also like to thank my sister Renuka and my brother-in-law Sukumar for their belief in me and their affection. They had a leading role in encouraging me to come to the United States to get a Ph.D degree.

My husband, Srikanth has been patient and understanding during the last year of my graduate school. His love and faith in me has been a motivation for me to work hard. I would like to thank my grandmother-in-law, Mrs. Savithri, mother-in-law, Mrs. Rajam Rajappa and my sisters-in-law and my brothers-in-law for their encouragement.

My friends in the local community have made me feel like a 'home away from home.' I thank Ramanujam, Kalyani, Sangeetha, Chak and Madhu, John and Helen, Apple Oxman and her sons, daughters-in-law and family, in particular, Cam, Mike and Lisa.

I gratefully acknowledge the assistance of all the staff in the Chemistry department at Oregon State University who have made my stay in Corvallis very pleasant. I also enjoyed working with Dr. Krueger and the undergraduate students at Oregon State University as a Teaching Assistant. I thank the department for providing me such an opportunity.

I would also like to acknowledge the encouragement of my friends and Teachers in India and the United States who had immense faith in my capabilities and encouraged me to pursue my dreams.

TABLE OF CONTENTS

LIST OF FIGURES

LIST OF TABLES

COMPLEX OXIDES OF 6p BLOCK ELEMENTS

CHAPTER 1:
INTRODUCTION

Post-transition metals chemistry

Oxides of post-transition metals have a variety of interesting properties, many of which are related to the fact that they have two stable oxidation states: s^0 and s^2. Complex oxides containing Bi, Tl and Pb form superconducting materials with high critical temperature. This could be attributed to their exhibiting mixed valency, $6s^0 + 6s^2$, or the disproportionation reaction:

$$6s^1 \rightarrow 6s^0 + 6s^2$$

Materials with useful optical properties and ferroelectric properties have also been made using these elements. This dissertation involves the synthesis and characterization of some of these heavy metal oxides.

Superconducting materials

Numerous systems involving oxides of transition and post-transition elements have been studied in the recent years in search of superconducting properties. The search for new oxide systems has been based on the features observed in the compounds already synthesized. For example, properties like mixed valency, a metal-insulator transition or geometry preferred by a cation seem to give a direction to proceed in order to synthesize new compounds and possibly increase the critical temperature of the exisiting compounds.

The critical temperature (T_c), the temperature below which the compounds become superconducting, has been the highest in copper-oxide based superconductors. The highest T_c in non-copper oxide superconductors

has been in the $(Ba,K)BiO_3$ system, where the T_c has been found to be up to 34 K (1, 2).

Superconductivity has been observed in non-oxide systems like intermetallics, sulfides, silicides, borides and more recently in borocarbides (3). Alkali metal doped fullerenes, for example K_xC_{60} has been found to be superconducting with T_c up to 33 K (4).

Examples of other oxide superconductors

Oxide bronzes, with the general formula A_xWO_3 are related to perovskite type structure. The WO_6 octahedra share corners to build up a three dimensional network. The A cation is usually an alkali or alkaline earth cation. When x is zero, the compound is insulating. Increasing values of x lead to metallic behaviour. Tetragonal and hexagonal tungsten bronzes are known to become superconducting e.g. $Rb_{0.3}WO_3$, Tc = 6.6 K (5).

$LiTi_2O_4$ has a spinel structure and exists over a range of composition, $Li_xTi_{3-x}O_4$. The highest T_c observed is 13.7 K for x ~ 1.0 (6).

Li_xNbO_2 phases are superconducting at 5 K. The starting material $LiNbO_2$ is a semiconductor (7); after deintercalation Li_xNbO_2, x = 0.45 - 0.5 phases are superconducting (8).

A list of oxides that are known to be superconducting are given in Table 1.1.

Table 1.1

Some known oxide superconductors

System	T_c, K	Reference
$SrTiO_{3-x}$	0.7	9
A_xWO_3 (A = Rb,Cs)	6	5
$BaPb_{1-x}BiO_3$ (0.35<x<0.15)	13	1
$Li_{1+x}Ti_{2-x}O_4$	13	6
$Ba_{1-x}K_xBiO_3$	34	2
Li_xNbO_2	5	8
$La_{2-x}M_xCuO_4$, M = Ca,Sr,Ba; x = 0.2	40	10
$LnBa_2Cu_3O_7$, Ln = lanthanide	90	11
Bi-Sr-Ca-Cu-O, 2212,2223	80,125	12
Tl-Ba-Ca-Cu-O, 2212,2223	80,125	13
Pb-Sr-(CaLn)-Cu-O,2213	70	14
$YBa_2Cu_4O_8$	80	15
$HgBa_2Ca_2Cu_3O_{8+\partial}$	134.5	16

$(Ba,K)(Bi,Pb)O_3$ superconductors

In the $Ba(Pb,Bi)O_3$ system, the highest Tc has been found to be 13K. The end members of the solid solution, $BaPbO_3$ and $BaBiO_3$ are both perovskites. $BaPbO_3$ is metallic due to the overlap of Pb 6s and O 2p bands. Neutron diffraction data indicated two kinds of bismuth in $BaBiO_3$, Bi^{III} and Bi^{V}, therefore it can be represented as $Ba_2Bi^{III}Bi^{V}O_6$ (17). The band structure comprises of the Bi 6s band moved up to the Fermi level and split due to the different Bi-O distances. Half the Bi 6s band is above the Fermi level (Bi^{V}) while the other half is below the Fermi level (Bi^{III}). Therefore, $BaBiO_3$ is a semiconductor, with the activation energy of conduction related

to the reaction, $Bi^{III} + Bi^{V} \rightarrow 2Bi^{IV}$ (18). In the $BaPb_{1-x}Bi_xO_3$ system, metallic properties are observed for the region x = 0.0 - 0.3. The highest Tc of 13 K was found for the composition x = 0.27(19).

There have been reports of Tc up to 37 K in $(Ba,K,Rb)BiO_3$, with a synthesis involving the preparation of the compound in a vacuum furnace (20). However, this preparation could not be reproduced in this laboratory. The preparation always resulted in the formation of $(Ba,K)BiO_3$, with a T_c of about 30 K (1).

Synthesis approaches for new phases

Attempts have been made to synthesize new mixed valent compounds of bismuth in other systems to explore possible superconductivity. Examples of such systems are the recent work on bismuth oxides using hydrothermal techniques and high pressure experiments using high oxygen partial pressure (21). Hydrothermal methods use water under pressure and temperatures above its boiling point at one atmosphere. Superconductivity has not yet been found in any other mixed-valent bismuth oxide system so far.

Preparative conditions could also be modified to synthesize new phases. Non-equilibrium techniques of synthesis could be used to synthesize phases that are not normally accessible through conventional solid-state routes. Low temperature synthetic routes can be used to synthesize metastable phases.

Recently, thallium based superconductors have been grown hydrothermally. Mixtures of $TlNO_3$, BaO, CuO, $CaCO_3$ along with H_2O_2 were subjected to hydrothermal synthesis at 160°, to yield the $Tl_2Ba_2CuO_6$ and $Tl_2Ba_2CaCu_2O_7$ phase along with other impurities (22).

The superconductor $(Ba,K)BiO_3$ has been grown by molten salt electrolysis techniques using a potassium hydroxide medium (23). A copper compound in a high oxidation state, $NaCuO_2$ has also been synthesized by this technique (24). Therefore this technique is promising to synthesize new compounds with mixed valent cations. The silver oxynitrate compound, $Ag^{I}(Ag_2^{II}Ag_4^{III})O_8NO_3$ and the corresponding oxyfluoride compound, $Ag^{I}(Ag_2^{II}Ag_4^{III})O_8F$ were synthesized by the electrolysis of aqueous solutions of silver nitrate and silver fluoride respectively (25). The T_c of these mixed valent silver compounds are between 1 to 2 K. These are some examples of compounds formed by anodic oxidation. Analogous to the two dimensional cuprate superconductors where Cu^{II} and Cu^{III} form corner shared square planar CuO_4 units, corner linked AgO_4 square planar units are found in the three dimensional structure of Ag_7O_8X phases.

Electrolytic reduction of transition metal oxides has been studied extensively. Electrolysis of fused salts was first used by J.L. Andrieux and co-workers (26) to synthesize well-crystallized products for many transition metal oxides like vanadium oxide spinels. Transition metal sulfides, phosphides, silicides, borides and bronzes of tungsten and molybdenum were grown as large single crystals for the first time by cathodic reduction (27).

Hydrothermal methods have been employed to explore the possibility of making new compounds . These compounds may not be accessible by conventional solid-state synthesis routes. Some of the reactants are partially soluble in water under pressure. This enables reactions to take place at lower temperatures. This method could therefore be used to synthesize phases that are unstable at higher temperatures. Large single crystals of commercially useful compounds like quartz, corundum and ruby have been prepared by using hydrothermal techniques (28).

Applications of Bi(III) oxides

Oxides containing Bi(III) have been found to have many useful properties. Bismuth molybdates are of industrial importance as selective oxidation and as ammoxidation catalysts (29). The catalytic activity was related to the cation and anion vacancies. The bismuth molybdates, $Bi_2Mo_3O_{12}$, $Bi_2Mo_2O_9$, and Bi_2MoO_6, are known to be catalysts for the partial oxidation of hydrocarbons (30).

Bismuth vanadate, $BiVO_4$, is known for its ferroelasticity and oxygen ionic conductivity (31).

Bismuth silicate, $Bi_{12}SiO_{20}$ is photorefractive and has potential application as optical components in light modulators and reversible holographic storage media (32, 33). Cr and Mn doped $Bi_{12}SiO_{20}$ have been known to have a strong photochromic effect (34).

Bismuth germanate, $Bi_{12}GeO_{20}$, is strongly optically active; an applied electric field induces both linear and circular birefringence. The crystal is also strongly piezoelectric and photoconductive in the visible range (35).

A non-linear optical compound $BiCa_4V_3O_{13}$ has been synthesized (36) in this laboratory.

New Oxides of Bi(III) synthesized by low temperature hydrothermal synthesis

During the search for new mixed-valent bismuth oxides, some new Bi^{3+} compounds were synthesized. Chapter 3 describes one such compound made, which is a chromium bismuth oxyhydroxide. Another example of a Bi(III) compound synthesized by the hydrothermal method is the new oxyhydroxide, (La,Bi)OOH (37).

The lanthanum bismuth oxyhydroxide was isolated in the single crystal form and found to have the PbFCl type structure. The cation in this structure is in eight-fold coordination and may be divalent, trivalent or tetravalent. Substitutions on the F and Cl site with a variety of anions are known (38). However, this is the first compound with complete OH substitution on one site. Important applications of compounds with the PbFCl structure include luminescence and catalysis (39).

The structure of $La_{0.26}Bi_{0.74}OOH$ is essentially that of tetragonal PbFCl which has a space group of P4/nmm. However the space group for $La_{0.26}Bi_{0.74}$ OOH is Pmm2. The lowering of symmetry from tetragonal to orthorhombic space group is entirely due to an ordering of La into just one of the two layers making up the double layer. Hydrogen bonding cannot account for the distortion because of oxygen-oxygen distances being greater than 3.0Å. Thus by using a low temperature synthesis, a new compound with features not observed previously in this crystal structure type has been prepared.

A view of the unit cell and the coordination environment of the La^{3+} and Bi^{3+} are given in Fig 1.1 and Fig 1.2 respectively.

Chapter 2 discusses using electrodeposition of molten salts and aqueous solutions for synthesizing new phases. Some of these phases cannot be synthesized using conventional solid state techniques. Single crystals of these new phases can be easily grown by electrodeposition. Single crystals of $KBiO_3$, a Bi(V) oxide were grown for the first time. Conditions for deposition were established by means of cyclic voltammetry. Exploration of electrolysis of aqueous salt solutions for synthesis of new phases is also discussed.

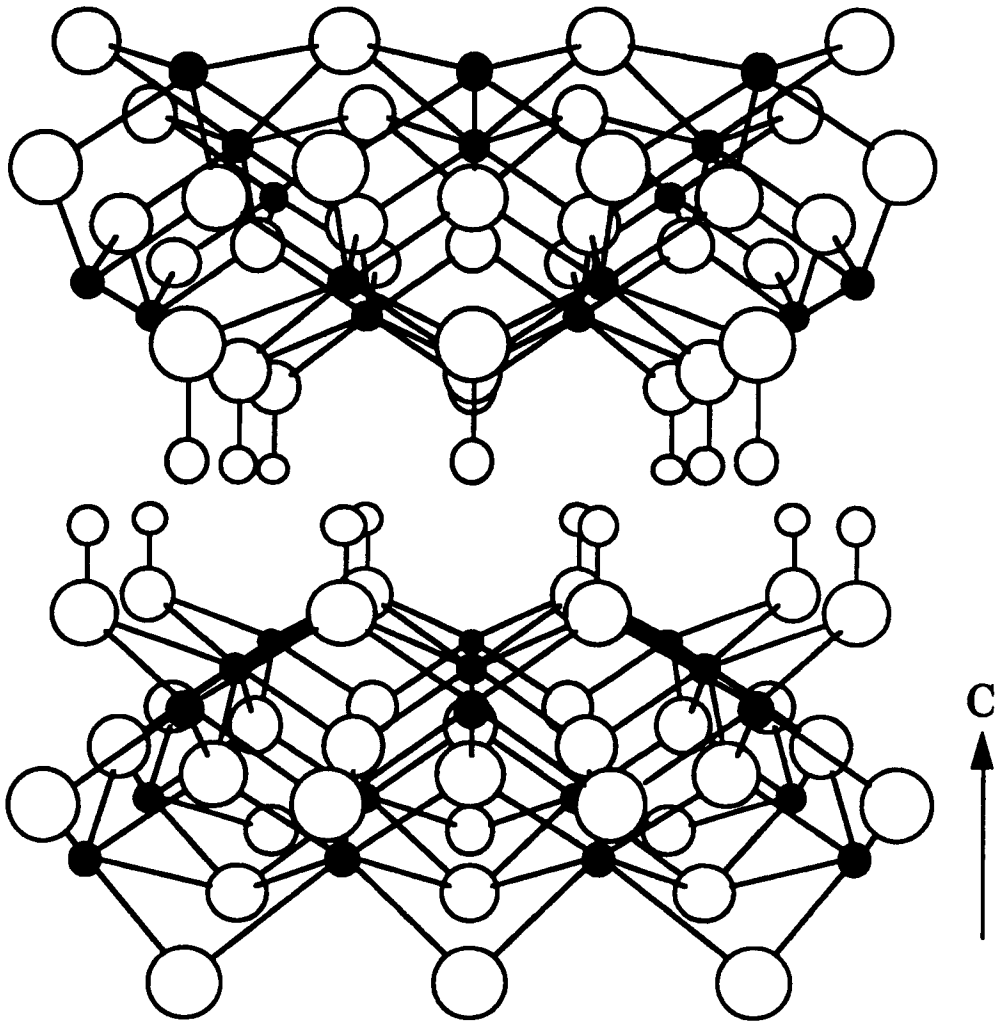

Fig 1.1 Crystal structure of $La_{0.26}Bi_{0.74}OOH$. Shaded circles are La,Bi(1), black circles are Bi(2), large open circles are oxygen and small open circles are H.

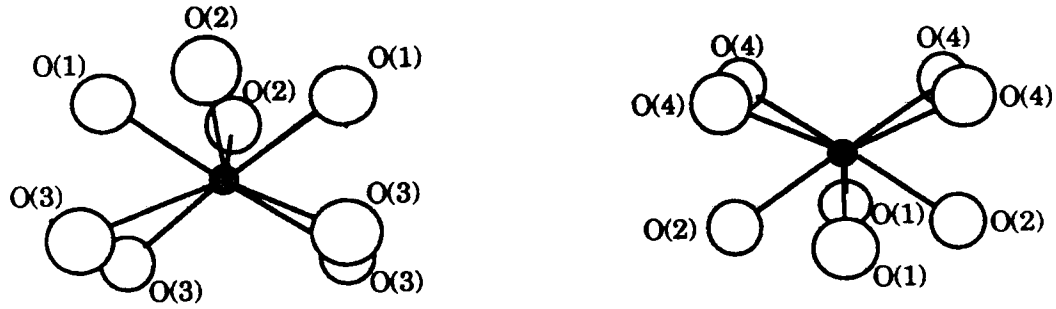

Fig 1.2 Coordination environment of Bi(1), La and Bi(2). Shaded circle represent Bi(1) and La; black circle represents Bi(2)

Chapter 3 discusses the synthesis of new bismuth oxides by low temperature hydrothermal synthesis. New bismuth oxides were synthesized by starting with a Bi(V) or Bi(III,V) compound. The structural features of a new mixed valent bismuth cadmium oxide has been examined by powder X-ray diffraction. The reason for the formation of a fluorite type structure in this system, unlike the pyrochlore structure of the alkali and alkaline earth mixed valent bismuth oxides prepared by similar methods, has been analyzed.

Chapter 4 discusses the synthesis and characterization of a new chromium bismuth oxyhydroxide. Low temperature hydrothermal synthesis has yielded the new structure type. The crystal structure of this new compound was determined by single crystal x-ray diffraction. The bond valence approach has been used to predict the possible location of hydrogen atoms. The new structure is also compared with a known bismuth chromium oxyhydroxide.

Chapter 5 discusses the systematic studies of $Tl_2Nb_2O_{6+x}$. The oxygen content of the compound varied with preparative conditions. Possible non-stoichiometry at the Tl site of the pyrochlore and the oxygen content was investigated by conducting neutron diffraction on powder samples of $Tl_2Nb_2O_{6+x}$ prepared under various conditions. Introduction of additional oxygen causes mixed valent Tl to exist, $Tl^{I}_{2-x}Tl^{III}_{x}Nb_2O_{6+x}$. Samples with varying oxygen content were synthesized and their structure refined using the Rietveld method with neutron diffraction data. The structure refinement provided information about stoichiometry of the compound and the mixed valency of Tl.

CHAPTER 2:
SEARCH FOR COMPOUNDS WITH ELEMENTS IN UNUSAL OXIDATION STATES USING ELECTRODEPOSITION TECHNIQUES

Electrodeposition as a synthesis technique

Electrodeposition has been used for growing crystals and synthesizing new compounds by reduction of transition metal oxides in molten salts (27,30). New phases were synthesized and characterized. Synthesis of new phases or growing crystals of new phases by anodic oxidation has been relatively uncommon. In the recent years, single crystals of $(Ba,K)BiO_3$ have been grown by anodic oxidation of Bi_2O_3 in a melt containing KOH and $Ba(OH)_2$ (41). Other compounds have been synthesized with substitutions in the Bi site. For example, In, Cd, Pb, Sn and some rare earths have been substituted at the Bi site, and new mixed valent Bi compounds were electrodeposited (42). Another new mixed valence phase $Ba_{3.12}K_{0.66}Bi_{3.37}Na_{0.63}O_{12}$ was synthesized using the same technique (43).

Complex salts of silver, $(Ag^{I})(Ag^{II}Ag^{III})_6O_8X$, $X = NO_3^-, F^-, BF_4^-$ phases have been grown by anodic oxidation of $AgNO_3$ or silver salt solutions (44). The oxide of silver, with silver in higher oxidation state, Ag_2O_3 was synthesized by the anodic oxidation of $AgNO_3$ solution at low temperatures in the presence of complex ions like ClO_4^- and PF_6^- (45). Mercury substituted silver oxide phases, $HgAg_6O_8X$ where $X = ClO_4^-$ and NO_3^- and $Hg_2Ag_{18}O_{33}H_{22}(ClO_4)_4$ were prepared by anodic oxidation of aqueous solutions of silver and mercury nitrates or perchlorates (46). These compounds were not superconducting. Silver metal forms at the cathode in all cases except in the case of fluoride solutions where Ag_2F forms.

The mixed valent bismuth compound $(Ba,K)BiO_3$ which is superconducting has been grown by electrodeposition. Pentavalent bismuth

compounds are difficult to obtain by conventional solid state methods. High oxygen partial pressures have to be used to obtain Bi(V) compounds or mixed valent bismuth compounds containing Bi(V). KLi_6BiO_6 (47), $Na_2Bi_4^{III}Bi^{V}AuO_{11}$ (48) and recently, ordered perovskites containing Bi^{V}, $Ba(Bi_{0.75}M_{0.25})O_3$ (M = Li or Na), $Ba(Bi_{0.67}M_{0.33})O_3$ (M = Mg, Ca, Sr, Ba, Cd or Cu) (21) have been prepared by using such synthesis conditions.

Sometimes molten hydroxides have been used to synthesize new Bi(V) oxides with alkali and alkaline earths but without high oxygen partial pressures (49). Oxide pyrochlores, $A_2BB'O_7$, A = La, Nd; B, B' = Pb, Sn, Bi have been synthesized using the low-temperature, ambient pressure, alkali melt route (50). Molten hydroxides are thus used as fluxes for synthesizing Bi(V) compounds.

In addition, electrodeposition by anodic oxidation has been used to oxidize Cu(II) to Cu(III). Thus a Cu(III) compound, $NaCuO_2$, has been synthesized (24) by electrolysis of a melt containing NaOH and $Cu(OH)_2$. $Ba(CuO_2)_2$ has been synthesized by electrolysis of a melt containing $Ba(OH)_2$, NaOH and $Cu(OH)_2$ (51).

Electrodeposition has been used to make thin films of superconductors (52, 53). In these cases however, the film formed by electrodeposition is post-annealed to obtain crystalline phases and superconductivity. Electrochemical method has been used for synthesizing a NbN precursor that is calcined above 600°C to yield superconducting NbN (T_c = 14.75 K) (54). AlN, which has some potential optoelectronic applications has been synthesized by a similar precursor route (55).

AMO_3 structure types

Perovskite structure

The most common structure type with the AMO_3 formula is the perovskite structure. In this structure, the MO_6 octahedra share corners to form a three dimensional network. This network is flexible and can distort readily to symmetries lower than cubic. The known $Ba(Pb,Bi)O_3$ and $(Ba,K)BiO_3$ superconductors have the perovskite structure (19, 56). The compounds prepared by electrodeposition with substitutions in the Bi site also have the perovskite structure (42, 43).

Pyrochlore structure

Another type of structure with a network of MO_6 octahedra is the pyrochlore structure. It is also ideally cubic and has the formula, $A_2M_2O_6O'$(57). The special position oxygen, O', is not essential for this structure. Therefore, there are a class of ABO_3 compounds called defect pyrochlores. Examples of such compounds are $AgSbO_3$ and $TlNbO_3$ (57).

Ilmenite structure

The ilmenite type structure is also well known for the general formula AMO_3. In this stucture, two-thirds of the octahedral interstices are occupied by the cations in a hexagonal cubic close packed array of oxide ions. $NaSbO_3$, $KSbO_3$, $LiSbO_3$ with the ilmenite structure have been prepared by solid state syntheses and ion-exchange reactions have been reported for these compounds (58).

Recently, structure predictions in the AMO_3 phase diagram has been reviewed (59). An approach for structural prediction based on the combination of ionic radii and bond ionicities is used in this review. A new

transition metal structure type, $InMO_3$, M = Mn, Fe has been explained and several compounds with this structure type have been predicted.

$KSbO_3$ type structure

One of the structure types with the general formula AMO_3 is the cubic $KSbO_3$ type structure. This structure is made of a network of edge and corner sharing octahedra of bismuth that form a three dimensional network of octahedra leaving channels running along the (111) direction (60). This network is illustrated in Fig. 2.1. The A^+ ions are free to move in these channels, and they are potentially good alkali ion conductors in a manner similar to ß alumina (61). Examples of such compounds are analogues of $KSbO_3$ where K^+ is substituted by Li^+, Na^+, Rb^+, Tl^+, Ag^+. Other examples of compounds with $KSbO_3$ type structure are given in Table 2.1.

Previous work on $KBiO_3$ and related bismuthates

Potassium bismuthate, $KBiO_3$, in the powder form has been synthesized previously. Oxidizing agents like Br_2, OCl^- were used in a alkaline medium to yield powder form of $KBiO_3.xH_2O$ (62, 63). $KBiO_3$ powder can also be prepared by using KOH melt around 200°C to ion-exchange with commercially available $NaBiO_3.xH_2O$.

A compound with the complex formula, $(K_{1.14}Bi^{3+}_{0.37})(Bi^{3+}_{0.27}Bi^{5+}_{1.73})(O_{5.71}\ OH_{0.29})$, with vacancies in the A site, having pyrochlore type structure is also known and has been studied for an uncommon thermally induced migration of cations (64, 65).

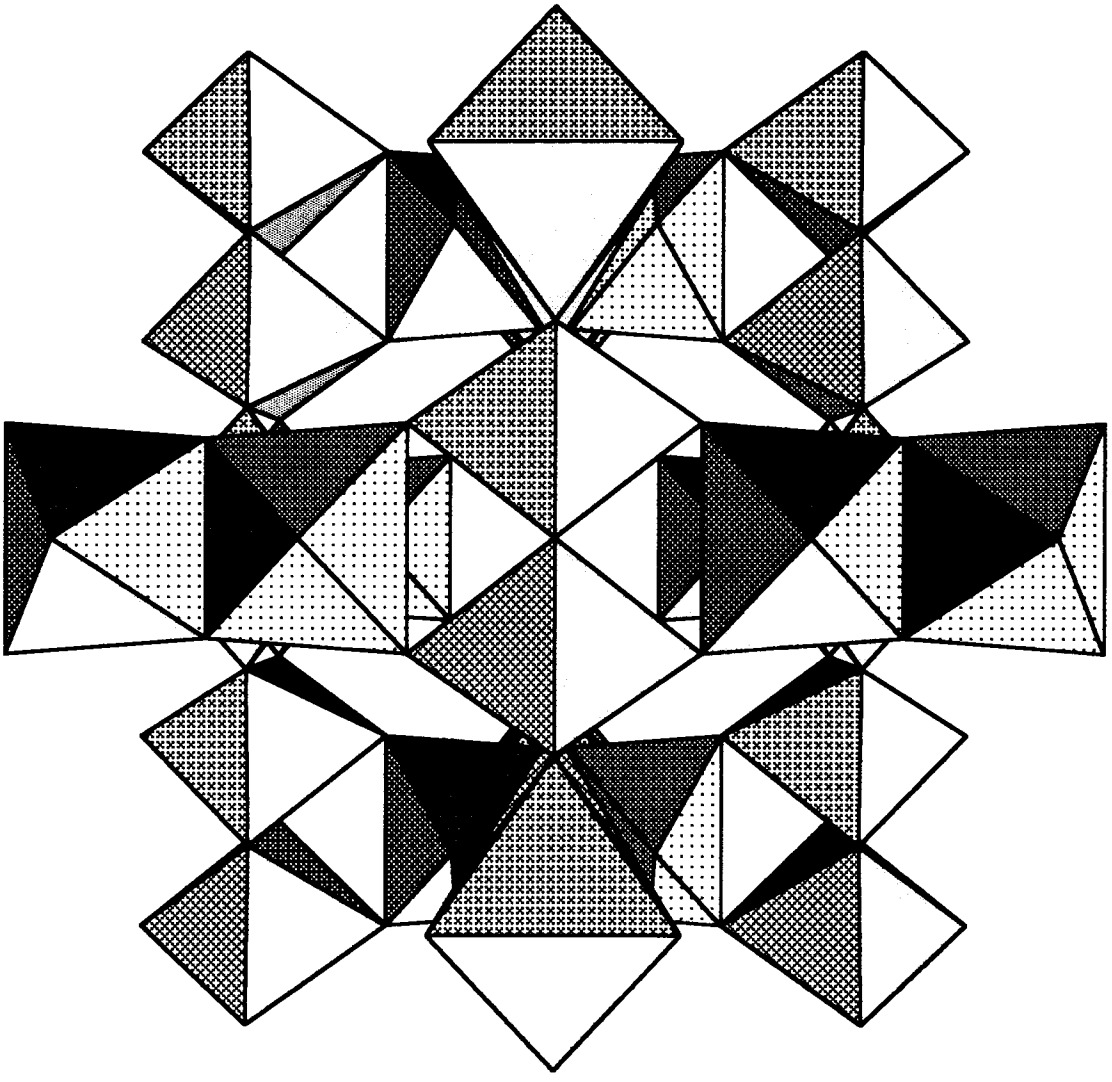

Fig 2.1 Network of MO_6 octahedra in $KSbO_3$ type compounds.
Figure shows the edge and corner sharing BiO_6 octahedra forming the network in $KBiO_3$

Table 2.1

Cubic $KSbO_3$-type compounds

Compound	**a, Å**
$KSbO_3$	9.56
$KBiO_3$	10.01
$RbSbO_3$	9.70
$NaSbO_3$	9.38
$LiSbO_3$	9.466
$AgSbO_3$	9.40
$NaOsO_3$	9.36
$KIrO_3$	9.487
$La_4Re_6O_{19}$	9.031
$Bi_3GaSb_2O_{11}$	9.491
$Bi_2LaGaSb_2O_{11}$	9.51
$Bi_2GdGaSb_2O_{11}$	9.46
$Bi_2AlSb_2O_{11}$	9.45
$Bi_3Ru_2SbO_{11}$	9.42
$Bi_3Fe_{1.67}Te_{1.33}O_{11}$	9.47
$La_3Ir_3O_{11}$	9.499
$Bi_3Ru_3O_{11}$	9.302
$Bi_3Os_3O_{11}$	9.357
$Bi_3Pt_3O_{11}$	9.399
$BaIr_2O_6$	9.411
$BaOs_2O_6$	9.33
$SrOs_2O_6$	9.20
$SrRe_2O_6$	9.205
$SrIr_2O_6$	9.344
$SrRu_2O_6$	9.22

Experimental

Electrolysis experiments were conducted in a platinum crucible in which KOH pellets were melted around 200°C. In a typical experiment, about 20 grams of KOH(ACS grade) were melted and about 2 grams of Bi_2O_3(Aesar) were added to the melt. Cyclic voltammetry was used to determine the potential at which electrolysis is performed. An EG&G Versastat was used to run cyclic voltammagrams and also to fix the potential at the point determined by the cyclic voltammograms. The electrodes used were typically 0.5mm - 1mm diameter wires of Au, Pt or Ag.

Nucleation begins soon after the application of desired potential determined by cyclic voltammogram. Cube shaped crystals with various colors were deposited anodically. Transparent red, dark-red and black colored crystals were obtained. These crystals were subsequently characterized by single crystal X-ray diffraction (66). The conditions for typical electrodeposition experiment are given in Table 2.2.

Table 2.2

Typical conditions for the Synthesis of $KBiO_3$

Electrodes: silver, platinum, gold wires 0.5-1.0 mm diameter
Potential: determined by cyclic voltammogram versus silver, platinum or gold electrodes.
Electrolyte composition: 20g KOH 2g Bi_2O_3
Electrolysis temperature: 250°C
Crystals of $KBiO_3$ deposited at anode

Cyclic voltammetry

Cyclic voltammetry has been used as a qualitative tool in analyzing mechanisms of electrochemical reactions (67). It involves scanning the potential and measuring the current as a function of changing potential. Cyclic voltammograms give an idea about the reversibility of electrode reactions. Electrochemical reversibility means that the reaction is fast enough to maintain the concentrations of the oxidized and reduced forms in equilibrium with each other at the electrode surface. The equilibrium ratio at a given potential is given by the Nernst equation. The oxidation and reduction processes can be identified and can be attributed to the number of steps involved in the electron transfer.

Cyclic voltammetry has been used in mechanistic studies of a number of reactions at room temperature and in aqueous and non-aqueous solutions.

Studying the mechanisms of reactions in molten salt systems through cyclic voltammetry is quite recent. These have given an idea about the potential at which oxidation or reduction begins to take place. The $Ba(OH)_2$-Bi_2O_3-KOH system was studied (68) and the following reactions were proposed to occur based on cyclic voltammogram at a Pt electrode:

$$2Bi + 6OH^- \rightarrow Bi_2O_3 + 3H_2O + 6e^-$$

$$Pt + 2xOH^- \rightarrow PtO_x + 2xe^- + xH_2O$$

$$Pt + 2OH^- \rightarrow Pt(OH)_2 + 2e^-$$

$$Bi_2O_3 + 2OH^- \rightarrow Bi_2O_4 + H_2O + 2e^-$$

$$Bi_2O_4 + 2OH^- \rightarrow Bi_2O_5 + H_2O + 2e^-$$

Cyclic voltammograms on the KOH-Bi_2O_3 system have been run on mixtures equilibrated overnight to get reproducible voltammograms.

The rise in the current in scanning the positive potential region shows that Bi^{3+} in solution is oxidized to Bi^{5+}. The deposition potential is therefore chosen in that region. The presence of just one peak seems to indicate that the oxidation is a one step process. The cyclic voltammograms using Ag, Au, electrodes are shown in Figures 2.2 and 2.3. The could be:

$$Bi^{3+} + K^+ + 6OH^- \rightarrow KBiO_3 + 3H_2O + 2e^-$$

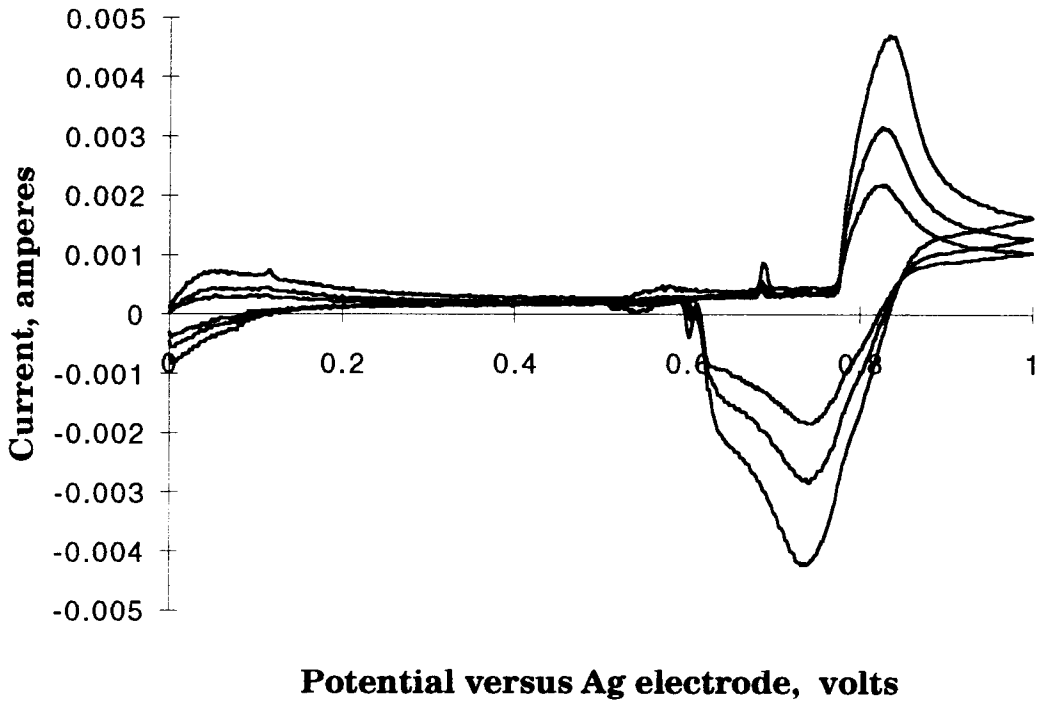

Fig 2.2 Cyclic voltammogram showing the oxidation of Bi^{3+} to Bi^{5+} in a KOH + Bi_2O_3 mixture at 250°C with silver electrodes. The various curves represent different scan rates starting with 100 mV/sec, 50 mV/sec, 20mV/sec respectively.

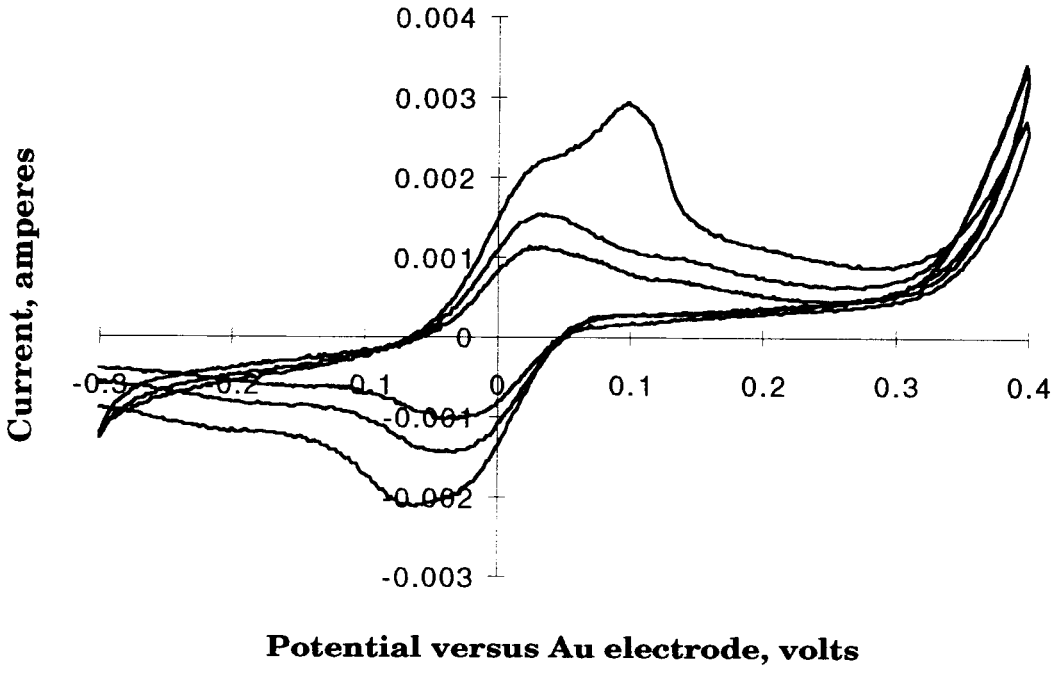

Fig 2.3 Cyclic voltammogram of KOH + Bi_2O_3 system at 250°C in a Au electrode.

The cyclic voltammograms in the case of Au and Pt electrode seem to be drawn out and the currents involved are in the order of microamperes. In the case of Ag electrodes, the current is higher and is the order of milli amperes. Furthermore, the reduction of Bi^{3+} to Bi metal, while scanning the negative potentials, seems to take place in two steps indicated by two peaks corresponding to this reduction as shown in Fig. 2.4. However, no deposition was observed at the lower reduction potential peak. Only bismuth metal was deposited at the electrode at the higher reduction potential.

Thus cyclic voltammetric studies have helped to fix the potentials at which electrolysis has to be carried out to enable the deposition of the desired compound. Constant potential and constant current depositions have been carried out to deposit crystals of Bi(V) compound.

Structural studies

Powder patterns obtained by grinding the crystals indicated that the products formed were indeed the $KBiO_3$ structure type as the lines indexed well with a body centered cubic unit cell and the lattice parameters were close to values reported in literature.

The microprobe data showed that the red crystals had a K:Bi ratio of 1:1. A transparent red crystal with approximate cubic shape about 0.05mm on an edge was used for collecting intensity data. Data were collected on a Rigaku AFC6R diffractometer using graphite monochromated Mo Kα radiation and based on a primitive unit cell, a = 10.022(2)Å. The data collection parameters are shown in Table 2.3. The intensities of three standard reflections were monitored every three hundred reflections

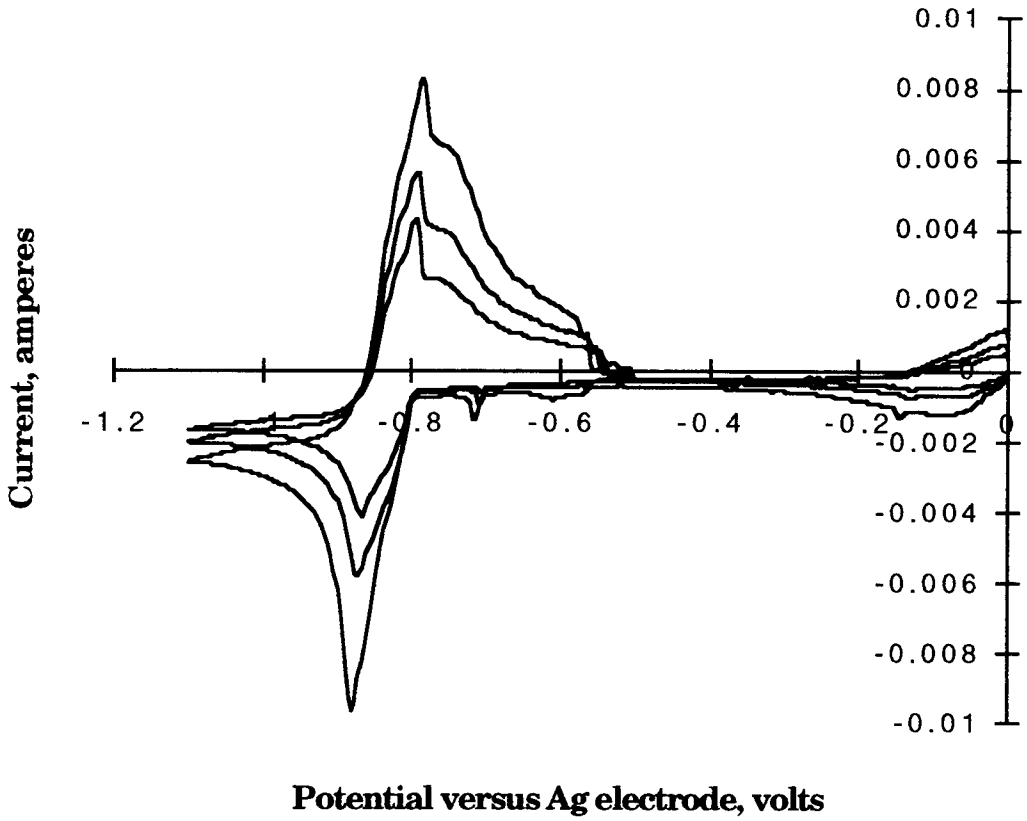

Fig 2.4 Cyclic voltammogram of KOH + Bi_2O_3 system at 250°C in a Ag electrode; potential scan is in the negative potential region.

Table 2.3

Crystal Data and Intensity Collection for $KBiO_3$
(transparent red crystal)

Empirical Formula	$KBiO_3$
Formula weight (g/mol)	296
Crystal System	Cubic
Space group	$Im\bar{3}$
a (Å)	10.022(2)
V ($Å^3$)	1006.7(5)
Z	12
Diffractometer	Rigaku AFC6R
Radiation	MoKα (λ = 0.71073Å)
	Graphite monochromated
Temperature	23°C
Maximum 2θ (°)	60
Data Collected	0<h<14, 0<k<14, 0<l<14
Scan speed (degrees/min)	16
No. unique data	576
R	4.15
R_w	5.3

throughout the data collection, showed no significant variation. An empirical absorption correction was done based on a psi scan.

throughout the data collection, showed no significant variation. An empirical absorption correction was done based on a psi scan.

A least squares refinement was initiated in the Im $\bar{3}$ space group assuming the ideal cubic $KSbO_3$ structure for the BiO_3 framework. After refining the parameters associated with Bi, O(1) and O(2), a difference fourier revealed electron density at 0 0 0, 1/4 1/4 1/4 and x x x (x≈ 0.34). These were then considered as positions for potassium and oxygen associated with water of hydration. The peak at x x x refined as a potassium atom. The occupancy of this site refines to 74.0%. This accounts for all potassium required for a $KBiO_3$ formula. The scattering power at 0 0 0 refined well as an oxygen atom. The electron density peak at 1/4 1/4 1/4 site was less than one oxygen atom. However a potassium atom was used to account for electron density at this site. The occupancy of a potassium atom at this site refined to 33.6%. Thus the single crystal X-ray data gave a formula for $K_xBiO_3.yH_2O$, x = 1.23, y = 0.17. The presence of excess alkali ions indicated by structural refinements has also been observed in sodium ß-alumina (69), with about 29% excess sodium and in $NaSbO_3$ (61), where a 28.7% excess sodium concentration was observed. The final refinement used anisotropic thermal parameters only for bismuth. The positional and thermal parameters are given in Table 2.4. Some interatomic distances and angles are given in Table 2.5. The coordination environment around Bi and K are given in Fig. 2.5.

After our publication, T.N. Nguyen et al. (70) also reported the crystal structure of this compound grown by electrodeposition also. The potassium atoms were located in three partially occupied crystallographic sites, two along the tunnels and one at the origin. Their stoichiometry obtained from microprobe data gave no indications of water of hydration. The electron

Table 2.4

Atomic and Isotropic Thermal Parameters for $KBiO_3$

Atom	**x**	**y**	**z**	**B_{eq} (Å)^2**
Bi	0.8399(1)	0	0.5	0.21(4)*
O(1)	0	0	0.359(2)	0.1
O(2)	0.337(1)	0.289(1)	0	1.0(3)
K(1)	0.3425(7)	0.3425	0.3425	3.7(5)
O(3)	0	0	0	1.0**

*$B_{eq} = (8\pi^2/3)S_iS_jU_{ij}a^*_ia^*_ja_ia_j$; anisotropic values given below

** Fixed parameter

ATOM	**U11**	**U22**	**U33**	**U12**	**U13**	**U23**
Bi	0.0027(5)	0.0037(5)	0.0017(5)	0	0	0

Table 2.5

Bond Distances (Å) and Angles(°) for $KBiO_3$

Bi	O1	2.12(2)×2		K	O2	2.72(2)×3
	O2	2.08(2)×2			O1	3.04(2)×3
	O2*	2.11(2)×2				

O2-Bi-O2	179(1)	O1-Bi-O2	90.5(5)
O1-Bi-O2*	169.5(8)	O1-Bi-O2*	87.6(8)
O2*-Bi-O2*	103(1)	O1-Bi-O1	82(1)
Bi-O1-Bi	98.2(6)	Bi-O2-Bi	128.4(6)
Bi-O2*-Bi	127.5(6)		

*O2 in plane with O1

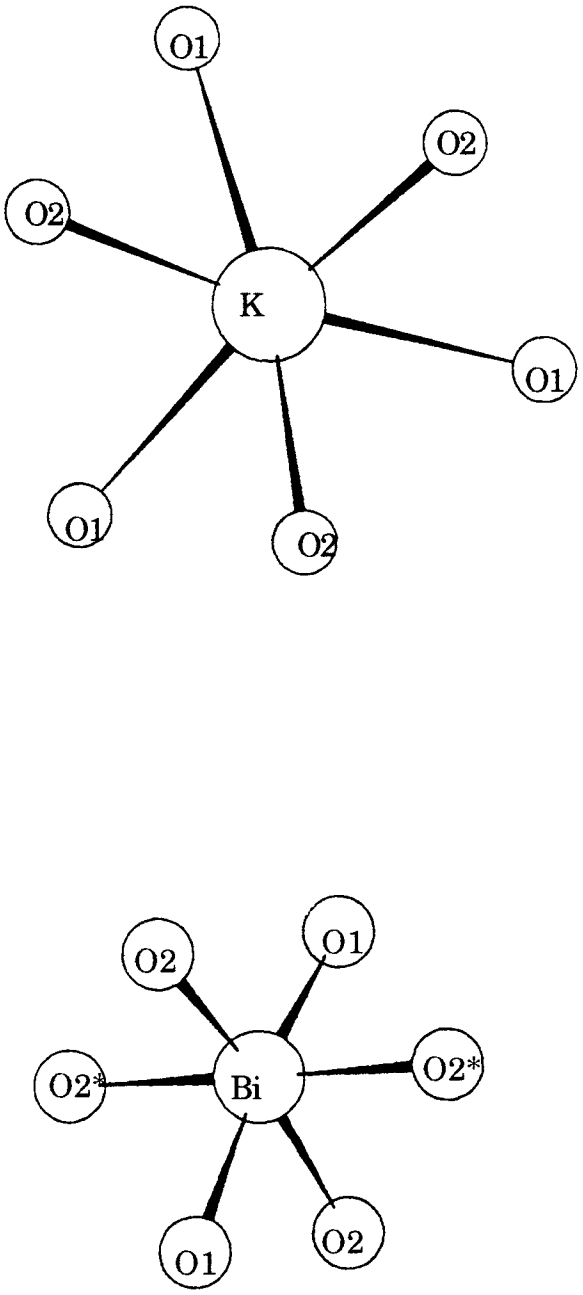

Fig 2.5 Coordination environment of K and Bi

density at the origin also refined well as a potassium atom in their single crystal data unlike our results in which it refined well as an oxygen atom which we associated with a water of hydration. The TGA measurement on our crystals also showed a small amount of water. This corresponds to about 0.8% of the sample, giving rise to the formula, $KBiO_3.0.2H_2O$.

Discussion

Unlike the perovskite structure, the MO_3 network in the $KSbO_3$ type structure is rigid and distortions to lower symmetry classes are not reported. Another difference between the perovskite and $KSbO_3$ type structure is the M-O-M bond angle. In the perovskite structure, this angle is ideally 180° and does not deviate much from the value even in non-cubic perovskites. However in $KSbO_3$ structure, the M-O-M angles are not fixed by symmetry and are in the range of 95° to 130.°

The ideal space group for $KSbO_3$ structure is $Im\bar{3}$. However the actual space group for compounds with cubic $KSbO_3$ structure is often of lower symmetry than the ideal space group. The body centered space group of I23 is found for $La_4Re_6O_{19}$ (71), and the primitive space group Pn3 is reported for $KIrO_3$ (72) as well as in compounds of the formula $A_3M_3O_{11}$ (73). It is basically the ordering of the interstitital atoms in the MO_3 framework that reduces the symmetry from $Im\bar{3}$. In the single crystals of $KBiO_3$, data collected on some of the crystals suggested the presence of primitive reflections not allowed in the $Im\bar{3}$ space group. A precession photograph of one of the crystals, however, did not show the presence of these reflections. Therefore $KBiO_3$ was taken to be body centered cubic.

The edge sharing of octahedra in the cubic $KSbO_3$ structure causes this structure to be unfavorable compared to the perovskite structure based on

electrostatic considerations. This suggests that metal-metal bonding between metals of the M_2O_6 dimer might be the stabilizing factor to compensate for the electrostatic repulsion of the two metal cations in the dimer. Metal-metal bonding is present in some of the compounds with the cubic $KSbO_3$ structure. For example, one-sixth of the positions occupied by K^+ ions in $KBiO_3$ are occupied by OLa_4 groups in a framework built of ReO_6 octahedra the formula becomes $(OLa_4)Re_6O_{18}$ or $La_4Re_6O_{18}$. In this structure, there is Re-Re bonding within the edge sharing pairs of octahedra (Re-Re = 2.42Å). However there are compounds in the $KSbO_3$ type structure with no metal-metal bonding. In $KBiO_3$, the bismuth atoms in the M_2O_6 dimer are displaced away from each other as would be expected when no metal-metal bond is formed. For ideal octahedra, the Bi-Bi distance would be 2.97Å based on the average of the Bi-O distances in the table. The actual Bi-Bi distance is 3.21Å.

In $KBiO_3$, the M-O-M angles are 98° and 127°. The M-O-M angle of 180° found in the ideal perovskite structure is favored in the case when the M cation is a d^0 transition metal. In this case, overlap of the metal t_{2g} and oxygen 2p orbitals gives rise to a π bonding interaction. Thus, cations such as Ti^{4+} and Nb^{5+} prefer the perovskite structure over the cubic $KSbO_3$ structure. Electrons added to the d orbitals are antibonding with respect to the M-O-M π bonding linkage. Thus, as we proceed to the right in the periodic table, the cubic $KSbO_3$ structure becomes competitive with the perovskite structure despite unfavorable electrostatic repulsion of the metals cation in the M_2O_6 dimer. Bending of the M-O-M angles away from 180° converts the π antibonding electrons to nonbonding electrons. The M-O bond has less oxygen s character as the M-O-M decreases from 180°. Thus, the cost of sp hybridization is reduced.

Different cell edges have been reported in literature for $KBiO_3$ (74, 75). This could be related to the water of hydration present in the sample. Our structural analysis also suggests some water of hydration.

The opaque red crystals have slightly different cell edge than the transparent red crystals. The red color is due to the band gap and can also be considered to be due to a charge transfer transition: O2p to Bi 6s.

Other Systems studied by electrodeposition

The colors of crystals obtained by electrodeposition with different electrodes, varied from transparent red to opaque red. Intensity data was collected on both these type of crystals, and it was found that they had similar lattice parameters. When platinum electrodes were used, electron microprobe analysis showed that the crystals contained 0.02moles Pt in them in addition to K, Bi and O. Intensity data was collected on these crystals also. Black crystals had a K:Bi ratio of 2:3 as determined by the microprobe data. A single crystal X-ray diffraction analysis of the black crystals showed the presence of Bi^{3+} along with potassium in the potassium sites along the channels.

Electrolysis experiments were performed using NaOH, LiOH and RbOH separately and along with KOH at different melting temperatures. No electrodeposition was observed except when pure KOH was used. With $Sr(OH)_2$ + KOH, electrolysis yielded crystals which could be indexed as cubic. However, these results were not reproducible. The powder pattern of these crystals is shown in Fig. 2.6.

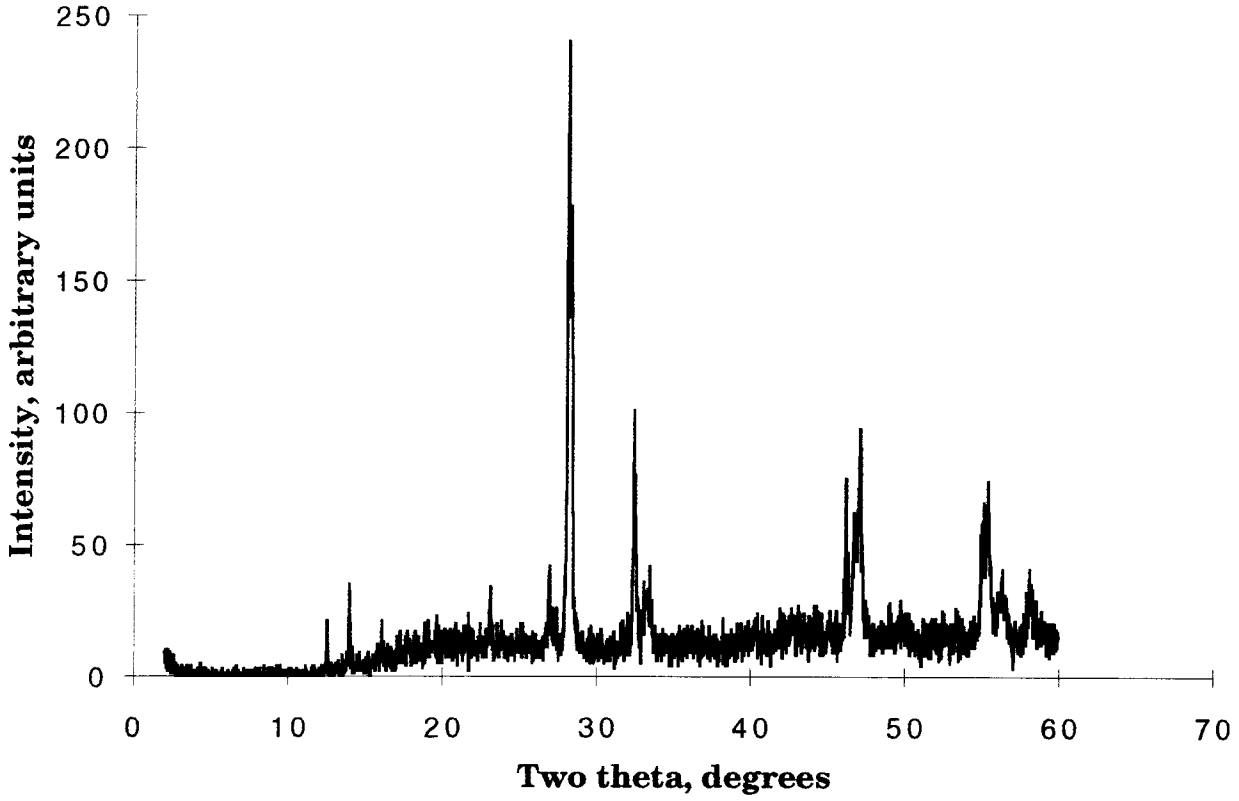

Fig 2.6 Powder pattern of crystals obtained by electrodeposition of melt containing KOH + $Sr(OH)_2$ +Bi_2O_3

Ion-exchange reactions of $KBiO_3$ crystals

Some alkali metal-early transition metal ternary oxides have been synthesized with layered and framework structures and shown to exchange alkali metal ions for protons in aqueous acids. Metastable oxide structures can also be prepared. For example TiO_2 (B) was prepared by the dehydroxylation of $H_2Ti_4O_9$ (76). Ion exchange reactions were pursued to explore the possibility of synthesizing new phases.

Ion-exchange reactions were tried using molten nitrates of Ag, Tl, Li, Na, Rb on $KBiO_3$ crystals. Decomposition of the $KBiO_3$ structure resulted. In the case of Ag and Tl, Bi^{5+} could be oxidizing Ag^+ and Tl^+ to higher oxidation states, resulting in a mixture of phases rather than a simple ion-exchanged product.

In the case of Ag^+ ion -exchange, an aqueous $AgNO_3$ solution was also tried. This resulted in an ion-exchanged product. The microprobe data showed that only 10% of the K^+ ions were replaced by Ag^+ ions. No K^+ could be detected by electron microprobe. Thus the formula of the compound is probably $Ag^+_{0.1}\ H^+_{0.9}BiO_3$.

The exchange of protons for K^+in $KBiO_3$ has already been reported in literature (77). The proton conductivity of the ion-exchanged product was also studied. It was found that $HSbO_3$ was a better proton conductor than $HBiO_3$ probably due to the higher basicity of the SbO_3 framework.

The ion-exchange of NH_4^+ ions for the K^+ ions have also been studied with $KSbO_3$(78). Similar reactions were tried with $KBiO_3$. The resulting product showed a shift in the lattice parameters as expected for an NH_4^+

exchanged product. However, it is not clear whether all the protons were exchanged by NH_4^+ ion.

Table 2.6 summarizes the results of ion-exchange reactions and the other compounds obtained by electrodeposition during the course of this study.

Ionic conductivity of $KSbO_3$ type materials

Since the materials with $KSbO_3$ type structure have alkali metal cations disordered in the tunnels formed by the other cation-oxygen framework, they could potentially have high alkali metal ion conduction.

The crystals of $KBiO_3$ grown by electrodeposition were studied for K^+ ion conductivity (70). The conductivity of $KBiO_3$, 10^{-5}S/cm at 300° C is 3 orders of magnitude lower than the reported conductivity of $NaSbO_3$.1/6NaF, 10^{-2}S/cm at 1kHz and 300°C. This difference was explained to be due to two different factors. One of them was thought to be due to the smaller size ratio of Na^+ and Sb^{5+} compared to K^+ and Bi^{5+}, while the remainder can be explained by the lower mobility of potassium ion compared to that of the sodium ion. The sodium ion has lesser role in stabilizing the framework structure due to the presence of the additional NaF in the structure, enhancing its mobility. The potassium ion is needed to stabilize the framework of Bi-O and is therefore not very mobile. It was speculated that the potassium ion mobility could be enhanced if species like H_2O could stabilize its structure.

Table 2.6

Lattice parameters of $KBiO_3$ and related compounds

Compound	**Color**	**Lattice parameter, Å**
$KBiO_3$	transparent red	10.022(2)
$KBiO_3$	dark brown	10.009(8)
Pt-phase	black	9.996(2)
$Ag_{0.1}H_{0.9}BiO_3$	black	~9.76
$HBiO_3.xH_2O$	red	~9.89
$NH_4BiO_3.xH_2O$	red	~9.86

Synthesis of new phases using anodic oxidation of aqueous solutions at room temperature

Compounds with mixed valent Ag in them have been synthesized by the electrolysis of aqueous solutions of silver. The typical formula of these compounds is $(Ag^{I})(Ag^{II},Ag^{III})_6O_8X$ where $X = NO_3^-, F^-$ depending on the type of silver salt used in the electrolysis (44, 45).

The structure of these compounds could be described based on a cubo-octahedral oxygen lattice with an O-O separation of 2.90Å. Two kinds of Ag ions are present. There are four silver ions with 8 oxygen neighbours on the apices of a cube (Ag-O = 2.52Å) and 24 silver ions with 4 oxygen neighbours at the corners of a square (Ag-O = 2.05Å). The eight coordinated silver ions could be Ag^{I} based on the known $Ag^{I} - O^{2-}$ distances. The other type of Ag ions should be a mixture of bivalent and trivalent silver ions (44). Fig. 2.7 illustrates the coordination environment of the silver ions in the compound.

Electrolysis experiments at room temperature were performed on solutions containing both $AgNO_3$ and $TlNO_3$. There was a black powdery deposition at the anode. The X-ray powder pattern showed an increase in lattice parameter in accordance with the larger sizes of Tl^+ and Tl^{3+} with respect to Ag^+ and Ag^{3+}. The cubic cell edge is 9.89Å, for the pure silver compound while it is ≈ 10.02Å for the mixed Ag, Tl phase. Fig 2.8 shows the X-ray powder pattern obtained. There was no evidence of a second phase from the powder pattern.

Electron microprobe analysis on the $(Ag, Tl)_7O_8NO_3$ sample revealed the presence of thallium, silver, nitrogen and oxygen. There were Tl rich regions and Ag rich regions in the product indicating inhomogeneties.

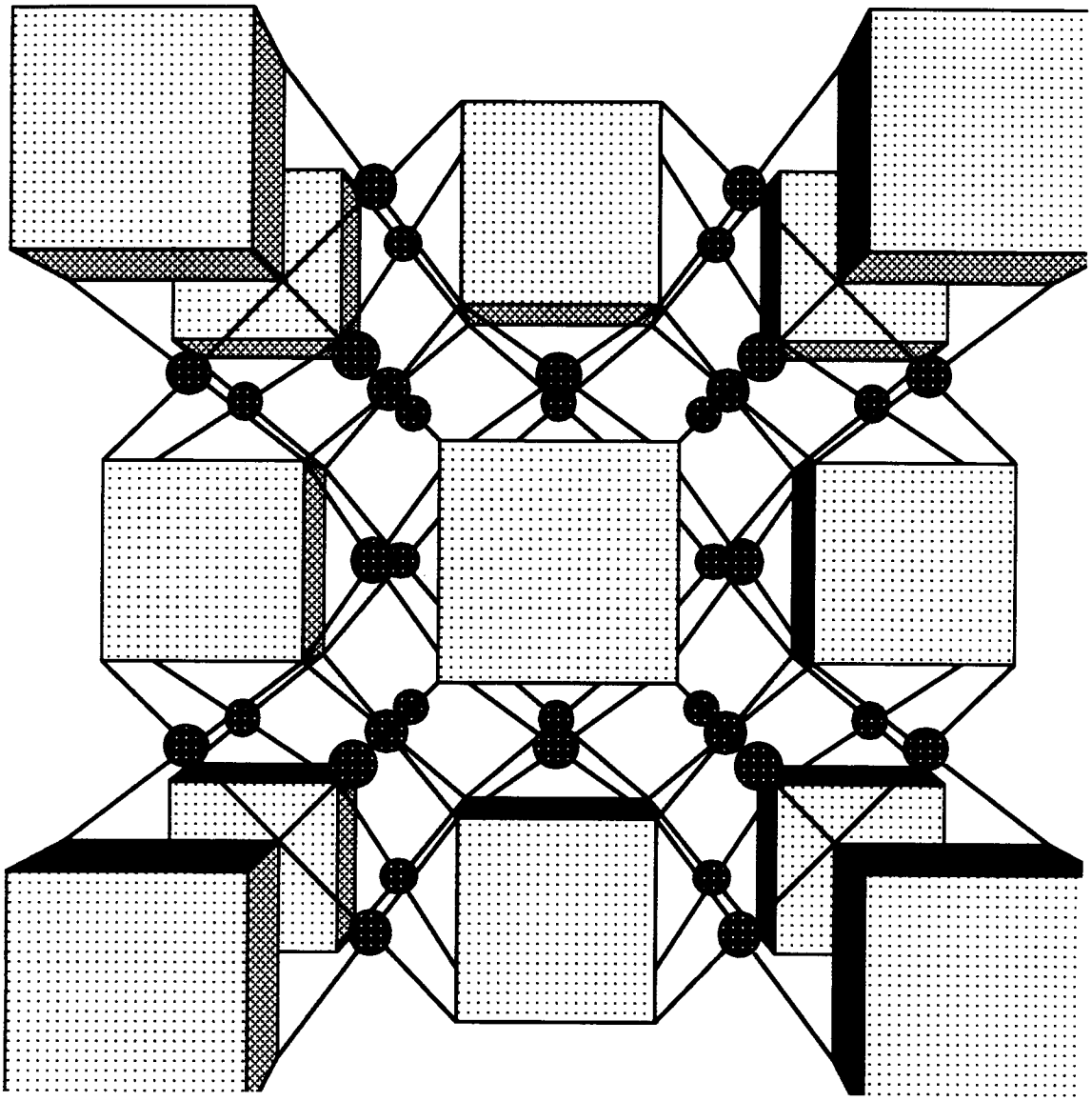

Fig. 2.7 Crystal structure of Ag_7NO_{11}. The cubes represent 8 coordinate Ag(I), dark circles show the 4 coordinate Ag(II,III)

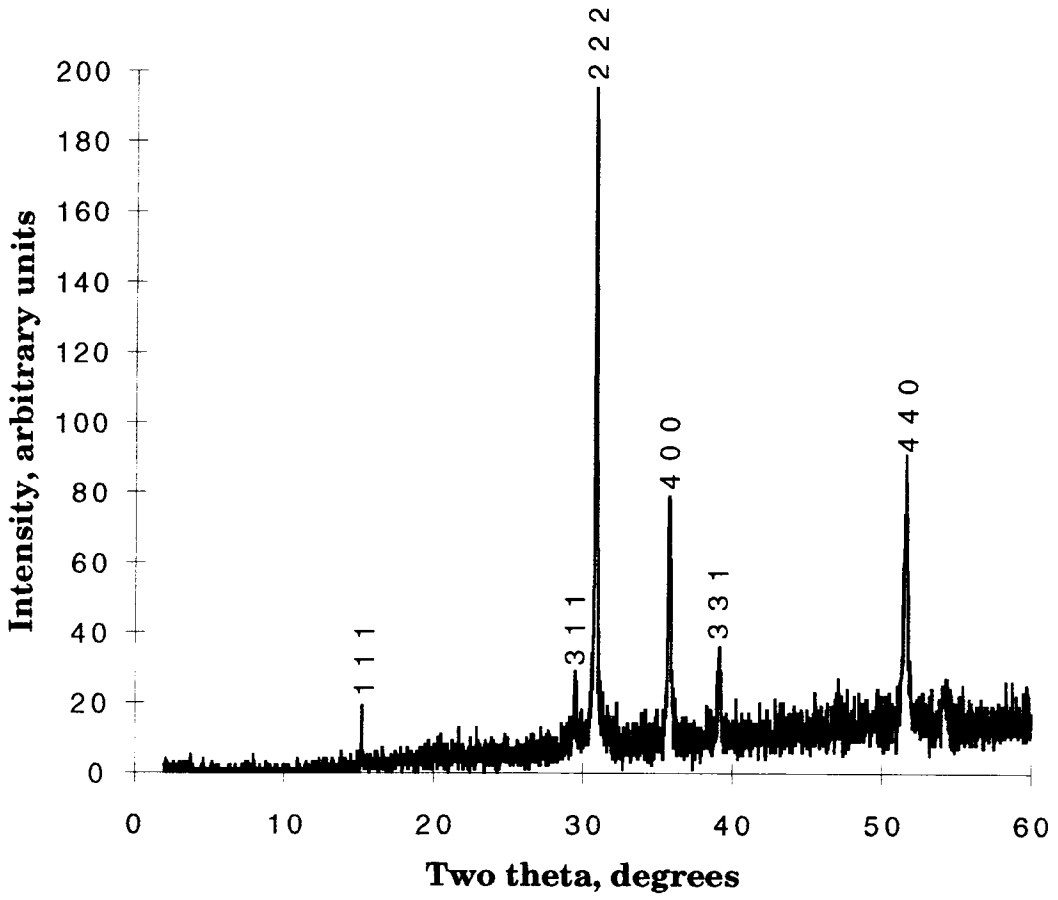

Fig 2.8 Powder pattern of the compound obtained by substituting thallium in Ag_7NO_{11}.

Compositionally homogeneous samples were attempted by changing the experimental conditions of electrolysis and concentrations of the electrolyte solution. Homogeneous products were still not obtained. However, most of the product had a Ag to Tl ratio of 5:2. This compound was not found to be superconducting down to 4 K. The $(Ag^{I})(Ag^{II,III})_6O_8NO_3$ compound is known to have a T_c of 1.25 K. Based on the observed powder pattern it could be speculated that Tl^{I} replaces Ag^{I} in the 8 coordinate site and hence the formula of the compound would be $(Tl^{I})(Ag^{II}, Ag^{III}Tl^{III})_6O_8NO_3$.

Table 2.7 shows the calculated powder patterns for the pure Ag and the mixed Ag,Tl compounds. The observed pattern is close to the calculated pattern based on the ratio given by the microprobe data. From the calculated pattern, the Tl substituted compound is close to the calculated pattern with Tl in the Ag(I) site. However, closely related phases with different Ag:Tl ratio may account for the lack of close correlation between the calculated and observed powder patterns.

Conclusions

Single crystals of $KBiO_3$ were grown for the first time using electrodeposition. In addition to Bi^{V}, the electrodeposition technique is promising to synthesize other oxidation states of bismuth. Single crystals of $KBiO_3$ helped to resolve some structural aspects like the variation in lattice parameter with the degree of water of hydration, delocalization of the interstitial site and the presence of Bi^{3+} in the potassium site in the Pt substituted potassium bismuth oxide. Room temperature electrolysis yielded a thallium substituted thallium silver oxynitrate, which was also synthesized for the first time.

Table 2.7

Observed and calculated powder patterns for thallium in Ag(I) site and in Ag(II, III) sites in Ag_7NO_{11}

H K L	**I_o**	**I_c, Tl in Ag(I) site**	**I_c, Tl in Ag(II, III) site**	**I_c, no Tl**
1 1 1	9.8	13.72	3.28	9.03
2 0 0	-	-	3.05	0.5
2 2 0	-	-	2.49	0.85
3 1 1	6.61	4.93	-	4.86
2 2 2	100	100	100	100
4 0 0	41.09	37.36	37.38	57.1
3 3 1	7.85	12.66	6.06	1.42
4 2 0	5.44	-	2.25	2.79
4 2 2	-	-	3.04	4.27
5 1 1	13.77	3.33	1.0	2.56
3 3 3	-	-	-	0.1
4 4 0	44.50	39.91	39.91	30.42
5 3 1	-	7.28	2.84	1.97
4 4 2	-	-	-	2.94
6 0 0	-	-	-	-
6 2 0	-	-	-	0.33

CHAPTER 3:
SYNTHESIS AND CHARACTERIZATION OF NEW BISMUTH OXIDES

Bismuth oxides are of interest because of several useful properties. Some mixed valent compounds of bismuth are known to be superconducting (19, 56). In addition, there has been a lot of work on the oxygen conduction properties of bismuth and bismuth-based oxides. A high ionic conductivity of $1\,\Omega cm^{-1}$ at 600°C could be obtained by the addition of lead oxide to bismuth oxide. This structure could not be quenched. Cooling always resulted in two metastable phases with different structures, depending on the composition (79).

Low temperature hydrothermal techniques have been recently used to synthesize new mixed valent alkali and alkaline earth bismuth oxides (80, 81). Therefore this technique was tried in an effort to synthesize other new bismuth oxides, mixed valent bismuth oxides, or metastable phases with interesting properties.

Bi(III) compounds in the Cd-Bi-O system are known (82, 83). These have been prepared by conventional solid state synthesis. An example of such a compound is $Bi_{(1-x)}Cd_xO_{(1.5-x/2)}$, x = 0.11 - 0.25 with the AgI type structure. However, no Bi(V) oxide or mixed valent bismuth compound is known in this system. Attempts to prepare the pyrochlore, $Cd_2Bi_2O_7$ using high oxygen partial pressures have not been successful (84). It was concluded that Bi(V) stabilization in the pyrochlore structure required higher basicity of the A cation .

The Cd-Bi-O system was explored to identify new phases in the low temperature region using hydrothermal synthesis for possible superconductivity.

Synthesis and decomposition

$NaBiO_3.x\ H_2O$ (Aldrich) and $Cd(NO_3)_2.4H_2O$ (Aesar) in a molar ratio of 1:4 were placed along with 75ml of water, in a teflon lined autoclave and heated for two days at 150°C. When the reactants were taken in a molar ratio of 1:1, 1:2, or 1:3 the products obtained had similar powder patterns. The brown product was filtered and air-dried. Electron microprobe analysis showed that the Cd:Bi ratio is 1:2. The product was characterized using powder X-ray diffraction. No sodium was found in the product.

The decomposition of this compound was studied by thermal analysis. There are two distinct weight losses occuring in the TGA. The first weight loss of about 6% occurs upto 450°C, which may indicate the presence of water and carbonate groups in the structure similar to the alkali and alkaline earth compounds prepared by low temperature hydrothermal syntheses. The second weight loss of about 2% completes around 600°C, resulting in a crystalline phase that could not be identified. This weight loss may be due to the loss of oxygen.

Structure determination

The alkali and alkaline earth mixed valent bismuth oxides prepared using hydrothermal synthesis are of the pyrochlore type (80, 81). The X-ray powder pattern of the title compound did not show any (odd,odd,odd) reflections characteristic of the pyrochlore structure. Based on a calculated pattern using LAZY PULVERIX the (odd,odd,odd) reflections are expected to be observable for the new cadmium bismuth oxide if it has the pyrochlore structure. A slow scan with longer counting times still showed no evidence of these reflections. Therefore Rietveld refinements were done based on a fluorite type unit cell.

Rietveld refinement of powder X-ray data of the mixed valent Cadmium Bismuth Oxide

The new mixed valent bismuth cadmium oxide was refined based on a fluorite type unit cell with mixed occupancy of Cd^{2+}, Bi^{3+} and Bi^{5+} on the cation site: $(Cd^{2+}, Bi^{3+}, Bi^{5+})O_{2-x}$. This was done using the Rietveld refinement program RIETAN (85) which gave R_I= 13.5%, R_p = 20.8%. The thermal parameter for the oxygen site was fixed (Table 3.1) because there was a high correlation between the thermal and occupancy parameters. The standard deviations on the refined parameters was not very low. The R factor was also not very low, probably due to three reasons. (1.) The background was quite high in the pattern collected. (2.) There seems to be a second phase with peaks very close to the predominant phase, apparently with a slightly different Cd/Bi ratio. (3.) There may be other atoms present in the compound like the oxygens from the OH or H_2O and the C and oxygens from the CO_3^{2-} that may have been left in the model apparently with a slightly different Cd/Bi ratio. The results of this refinement are given in Table 3.1, and the observed and the difference patterns are given in Fig. 3.1. These results show a closeness of the predicted model and the observed results.

Table 3.1

Positional and thermal parameters of $Cd_{0.34}(Bi^{3+},Bi^{5+})_{0.66}O_{1.67}$

a = 5.3895(4)

R_{wp} = 30.22% R_I = 13.51%

Atom	x	y	z	B	occupancy
Bi^{3+},Bi^{5+}	0	0	0	1.4(4)	0.67
Cd^{2+}	0	0	0	1.4(4)	0.33
O	0.25	0.25	0.25	4.0	0.7(4)

Iodimetric titrations

Iodimetric titrations were performed on the cadmium bismuth oxide. The solution was prepared by dissolving 0.5-1 gram of the powder in minimum amounts of concentrated hydrochloric acid. Some distilled water was added. About 1gram of KI was added. Since Bi^{5+} is a strong oxidizing agent, it oxidizes I^- to I_2. An iodine-starch complex forms a blue color. This was titrated against a standard thiosulfate solution. Using the disappearance of blue color, the end point was detected. The color of the solution still remains orange because the Bi^{3+}-I^- complex is orange in color. Subtracting the amount of Bi^{5+}, which is calculated by the equivalent of I_2 it liberates, from the total amount of bismuth present in the sample obtained by microprobe data, the amount of Bi^{3+} is also calculated.

Chemical analyses thus give a formula at $Cd_{0.34}(Bi^{3+}_{0.33},Bi^{5+}_{0.33})O_{1.67}$. The structure refinement is also in agreement with this formulation.

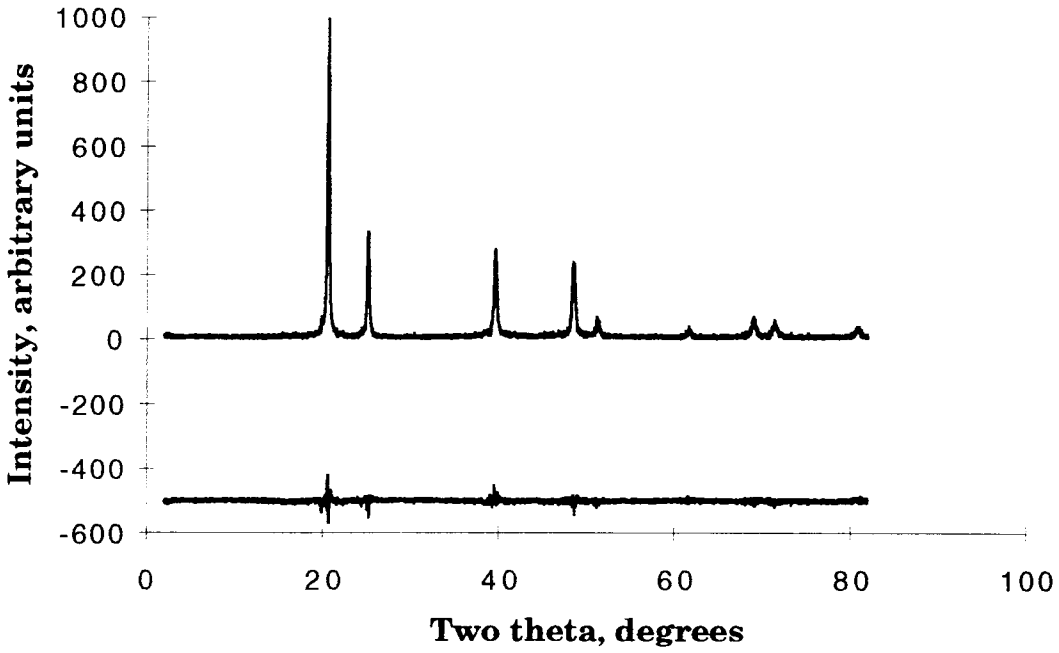

Fig 3.1 Rietveld refinement of cadmium bismuth oxide, showing the observed and the difference patterns

Results and Discussion

The alkali and alkaline earth mixed valent bismuth oxides prepared by similar methods had a pyrochlore type structure. The absence of superstructure reflections for the cadmium bismuth oxide gave an indication that the compound crystallizes in the fluorite type cell. The size of Bi^{3+} and Cd^{2+} are the same (radius of Cd^{2+} and Bi^{3+} is 1.10Å, radius of Bi^{5+} is 0.76Å). This has probably led to disorder of the two cations and hence a fluorite type structure. A comparison of the known compounds with the cadmium bismuth oxide is given in Table 3.2.

A mixed valent bismuth oxide in the Cd-Bi-O system has been synthesized for the first time. The reason for obtaining the disordered fluorite type structure has been analyzed.

The IR spectrum of $Cd_{0.34}(Bi^{3+}_{0.33},Bi^{5+}_{0.33})O_{1.67}$ did not show any absorption peaks in the region where pyrochlores normally have peaks, unlike the corresponding alkali and alkaline earth pyrochlores.

Table 3.2

Comparison of the cadmium bismuth oxide with known alkali and alkaline earth mixed valent bismuth oxides

$(A^+, Bi^{3+})(Bi^{3+}Bi^{5+})_2O_7$	r, Å	a, Å
$A = Sr^{2+}$	1.26	11.02(1)
$A = Na^+$	1.18	10.943(8)
$A = Cd^{2+}$	1.10	10.778(7)*

$r(Bi^{3+}) = 1.10Å$

* based on a fluorite type unit cell, a = 5.3895(4)

Attempts to prepare mercury and silver analogues of this compound were unsuccessful. Both attempts gave multiphase products. The Ag substituted product seemed to have a pyrochlore related compound along with other impurities.

Order-disorder in pyrochlore compounds

Infrared spectra of ordered and disordered pyrochlore type compounds in the rare earth oxide series $RE_2Ti_2O_7$, $RE_2Zr_2O_7$, $RE_2Hf_2O_7$ have been studied. The pyrochlore structure is expected to give a multitude of bands. The disordered structures with a statistical distribution of the cations and anion holes, accompanied by variation of bond distances and force constants tend to smooth out the spectra (86). The relationship between pyrochlore structure and fluorite structure is illustrated in Fig. 3.2.

Compounds of the type $A_2Pb_2^{IV}O_7$, were prepared by high pressure to stabilize high oxidation state and coordination number. Compounds with A = La, Pr, Nd, Sm, Eu or Gd were found to have the pyrochlore structure while when A is Tb, Dy, Ho, Er or Y the disordered fluorite structure is observed (87).

Plumbates with a formula, $A_2Pb_2O_7$ where A = Tl, Bi were prepared by solid state reaction under pressure in sealed gold tubes. The superstructure reflections (hkl all odd) were present in $Bi_2Pb_2O_7$ while they were absent in $Tl_2Pb_2O_7$. The similar size of Tl^{3+} and Pb^{4+} versus Bi^{3+} and Pb^{4+} accounts for the disorder and the missing superstructure reflections (88).

Thus based on the pyrochlore-fluorite transition in rare earth zirconates, titanates and plumbates, it can be concluded that the A:B size ratio governs the structure. When the sizes are very similar, the cations do not order and the disordered fluorite structure is found. There is also a

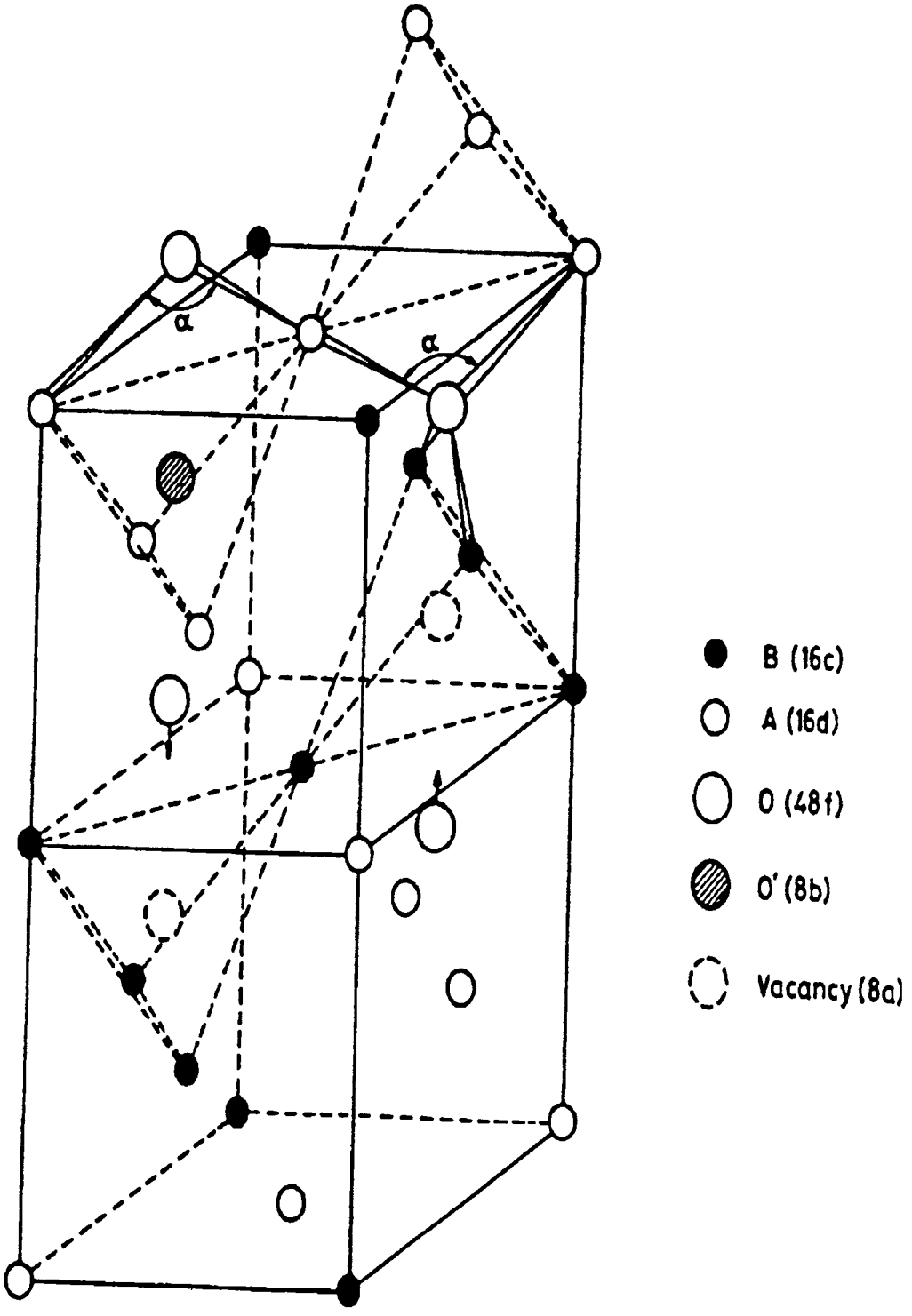

Fig. 3.2 The fluorite - pyrochlore transformation

correlation between the occurence of fluorite-type structure in $A_2M_2O_7$ when the corresponding MO_2 compound has a fluorite or fluorite-related structure (87). For example one of the forms of the mixed valent bismuth oxide, $(Bi^{3+}Bi^{5+})O_2$ is reported to have a fluorite related structure (89).

Other systems studied by hydrothermal reactions

The other systems tried in this search were $NaBiO_3$ in combination with $Pb(NO_3)_2$, $Al(NO_3)_3$, $Co(NO_3)_2$ and $BaBiO_3$ with $Cu(NO_3)_2$. All such preparations gave products with similar X-ray powder patterns. They could be indexed based on a tetragonal unit cell. Cell dimensions are close to each other with a ~ 3.5Å, and c ~ 8.6Å . Plate like crystals were obtained using $Al(NO_3)_3$. Single crystal data on them could not be collected since it was hard to isolate a good single crystal. Microprobe analysis showed that these white transparent crystals do not contain any Al in them. The sample was homogenous in composition with the Bi to O ratio of 2:3. The lattice parameters obtained based on a tetragonal unit cell does not match the lattice parameters of any known forms of Bi_2O_3. This could possibly be a new, low temperature form of Bi_2O_3 or Bi(O,OH) with a structure related to (La,Bi)OOH which was discussed in chapter 1. The powder patterns of the compound obtained are shown in Fig 3.3 - 3.5.

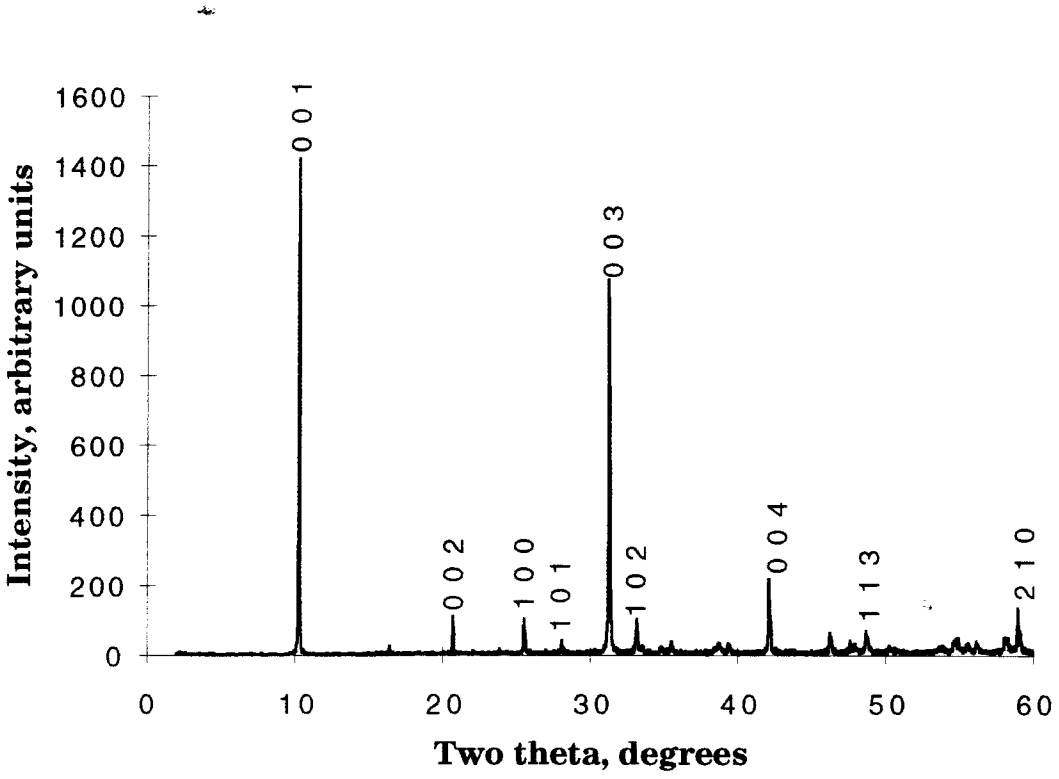

Fig 3.3 Powder pattern of product obtained by the reaction of $BaBiO_3$ with $Cu(NO_3)_2$

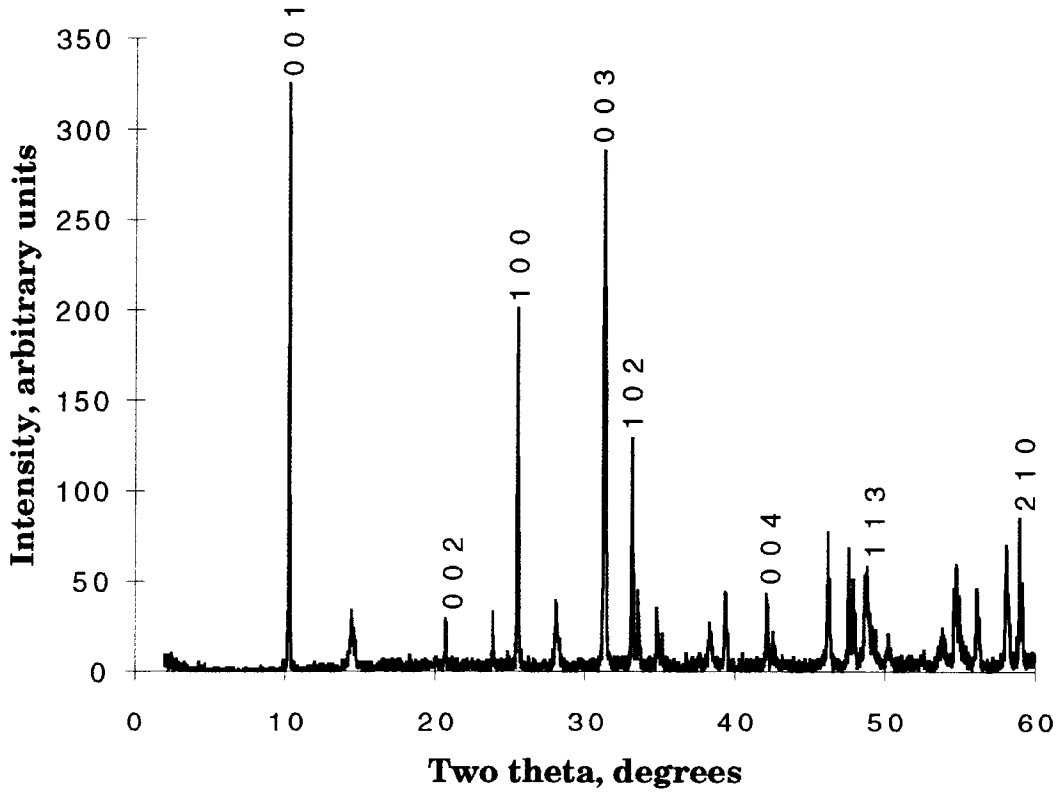

Fig 3.4 Powder pattern of product obtained by the reaction of $NaBiO_3$ with $Al(NO_3)_3$

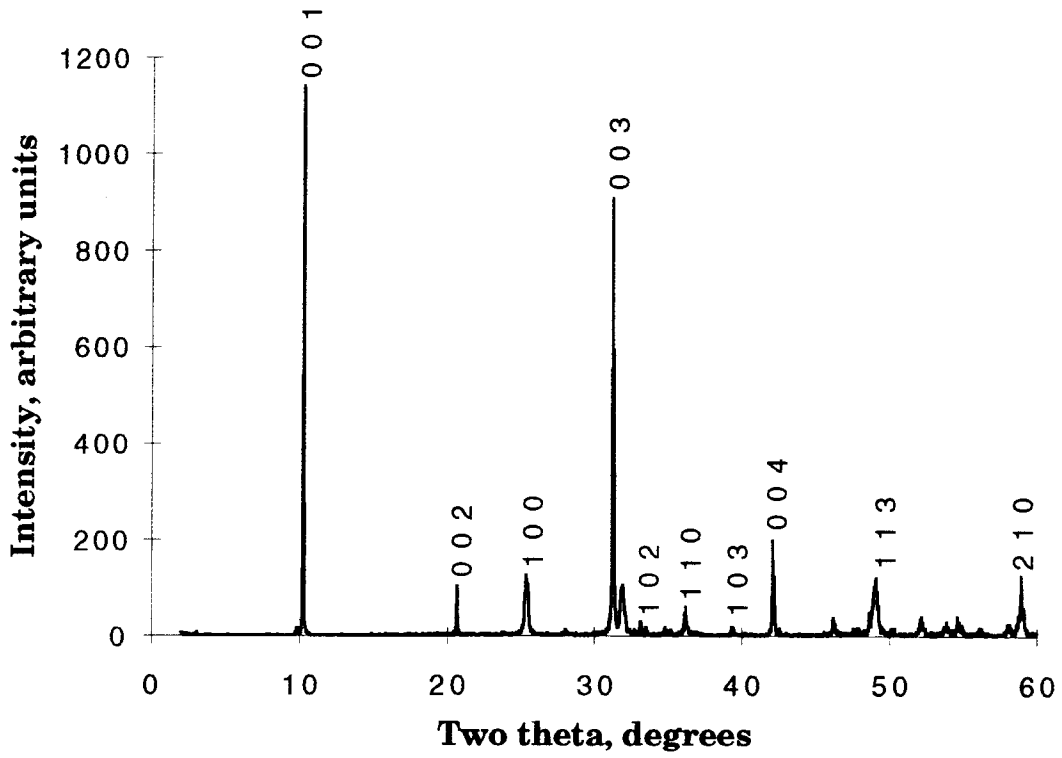

Fig. 3.5 Powder pattern of product obtained by the reaction of $NaBiO_3$ with $Pb(NO_3)_2$

Low temperature hydrothermal reaction of $HBiO_3.xH_2O$

Apart from using $NaBiO_3$ as the starting source of Bi, $HBiO_3.xH_2O$, which was prepared by exchanging for K^+ ions in $KBiO_3$ powder in 9M H_2SO_4, was also used as a source of Bi.

The brown product obtained by heating $HBiO_3.xH_2O$ in an autoclave could be indexed based on both a pyrochlore type unit cell and a fluorite type unit cell. The lattice parameters match the reported fluorite type Bi_2O_4. The powder pattern of the product obtained is shown in Fig. 3.6. The reported Bi_2O_4 with fluorite type structure has been prepared by applying high oxygen partial pressure up to 400 MPa to both amorphous and crystalline bismuth(III,V) oxide hydrates. The same study also reported the formation of Bi_4O_7 with a triclinic pyrochlore structure. This compound, Bi_4O_7 was found to be isostructural to $Bi^{III}_3Sb^{V}O_7$ which proves the existence of Bi^{5+} positions (89).

Recently, another form of Bi_2O_4 with ß-Sb_2O_4 type structure has been synthesized by low temperature hydrothermal method and its structure refined using neutron diffraction data (90).

Table 3.2 shows the bismuth oxides made by low temperature hydrothermal methods.

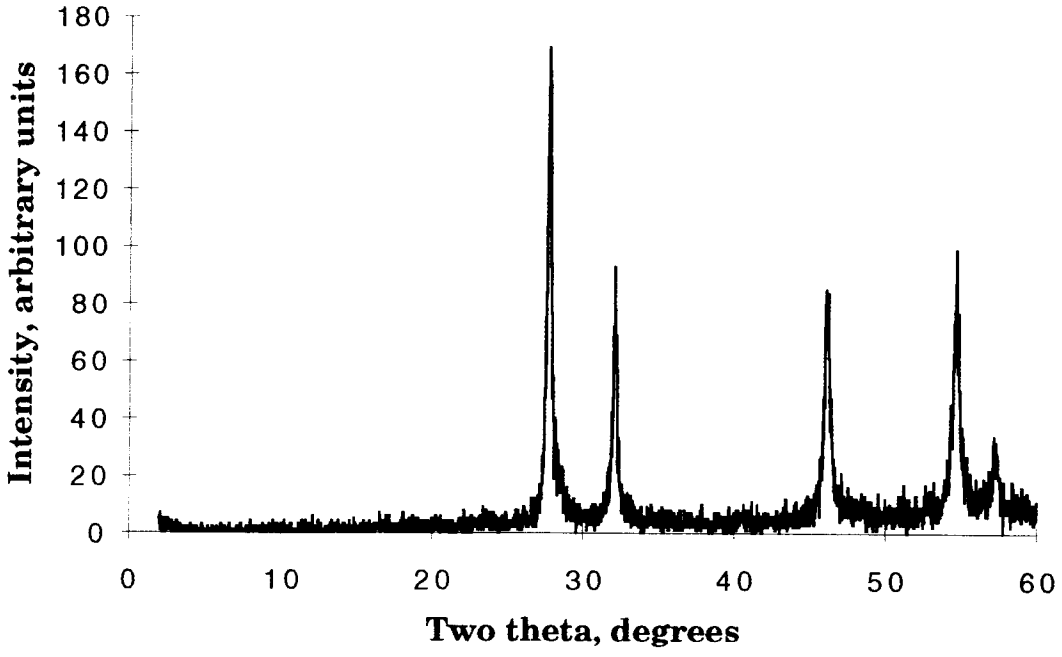

Fig. 3.6 Powder pattern of product obtained by the reaction of $HBiO_3.xH_2O$

Table 3.3

Bismuth oxides prepared by low temperature hydrothermal syntheses

Starting material	**compound**	**lattice parameters, Å**	**Reference**
$NaBiO_3$ + KOH	$Na_{0.39}Bi_{3.45}O_7$	a=10.943	70
$NaBiO_3$ + $Ca(NO_3)_2.nH_2O$[1]	$Ca_{0.66}Bi_{3.04}O_{6.7}(CO_3)_{0.10}$	a=10.77 b=10.90 c=10.92 ß=91.99	71
$NaBiO_3$ + $Sr(NO_3)_2.nH_2O$[2]	$Sr_{0.76}Bi_{3.13}O_{6.67}(CO_3)_{0.11}$	a=11.02	71
$NaBiO_3$ + $Ba(NO_3)_2.nH_2O$	$Ba_{0.68}Bi_{3.05}O_{6.41}$ $(H_2O,OH)_{0.59}$	a=11.09, c=10.92	71
$NaBiO_3$ + $La(NO_3)_2$	(La,Bi)OOH	a=3.808,b=3.811 c=8.600	28
$NaBiO_3$ + $Cr(NO_3)_3$	$HBi_3(CrO_4)_2O_3$	a=5.527 b=12.214 c=14.003 ß=92.95	Chapter 4
$NaBiO_3$ + $Cd(NO_3)_2.4H_2O$	$Cd_{0.34}Bi_{0.66}O_{1.67}$	a=5.8389	this work
$NaBiO_3$ + $Pb(NO_3)_2$	brown unidentified powder	a≈3.5 b≈8.6	this work
$NaBiO_3$ + $Al(NO_3)_3$	white plate like crystals,unidentified	a≈3.5 b≈8.6	this work
$BaBiO_3$ + $Cu(NO_3)_2$	black powder, unidentified	a≈3.5 b≈8.6	this work
$HBiO_3$	brown powder	a≈5.57	this work
$NaBiO_3$ + $LiNO_3$	Bi_2O_4	a=12.3668 b=5.1180 c=5.5670ß=107.84	80

1 Ca/Bi=0.25
2 Sr/Bi=0.25

Conclusions

A bismuth cadmium oxide with mixed valent bismuth was synthesized for the first time. The order - disorder phenomenon in pyrochlores has been analyzed with relation to the newly synthesized cadmium bismuth oxide. There is also an evidence for the formation of new bismuth oxides using low temperature hydrothermal synthesis.

CHAPTER 4:
CRYSTAL STRUCTURE OF $HBi_3(CrO_4)_2O_3$

Introduction

Phase equilibrium studies of the Bi/Cr/O system conducted in air report only the bismuth rich phases $Bi_{38}CrO_{60}$ with the Sillénite type structure and $Bi_{16}CrO_{27}$ (91, 92) However, $BiCrO_3$ with the perovskite structure is reported to form at high pressure (93, 94). Solution chemistry has given the bismuth-chromium oxyhydroxide $BiOHCrO_4$ (95, 96). The bismuth chromate, Bi_2CrO_6, is also reported (97). Apparently, no other bismuth-chromium oxides or oxyhydroxides are known.

A body centered cubic structure with the lattice constant a in the range of 10.10 to 10.25Å has been reported to form between Bi_2O_3 and various other metal oxides, for example with the oxides of Al, Si, Fe, Zr, Ce, Tl, Pb, B, P, Ti, V, Mn, Co, Ni, Zn, Ga, As, Rb, Nb and Cd (98).

Some of the common structure types of metal oxides containing Bi(III) are Bi_2WO_6, Bi_3TiNbO_9, $Bi_4Ti_3O_{12}$ which correspond to n = 1, 2,3 respectively of the Aurivillius family, with the general formula, $(Bi_2O_2)^{2+}[A_{n-1}B_nO_{3n+1}]^{2-}$ (99,100). These are layered perovskite related oxides. In Bi_2WO_6, bismuth is coordinated by five oxygens, four oxygens from the Bi_2O_2 layer and a fifth from the WO_4 layer. In the higher members, bismuth is eight coordinated with four oxygens from the Bi_2O_2 layer and four more from the perovskite slab at longer distance, giving rise to a distorted cubic environment around Bi^{3+}. $Bi_2Rh_2O_{6.8}$ and $BiCrWO_6$ form in the pyrochlore type structure (101, 102).

Some Bi^{3+} compounds are isostructural with those corresponding to those of La^{3+} as in halides and oxyhalides. Compounds with various La:Cr ratios in the lanthanum chromium oxyhydroxide system are known (103,

104). None of them are isostructural to the Bi^{3+} compounds with the same proportion of Cr. The compound described in this chapter has a structure that is different from any of the known La^{3+} or Bi^{3+} chromium oxyhydroxides.

Synthesis and decomposition

The reactants $NaBiO_3$(Aldrich) and $Cr(NO_3)_2 \cdot 9H_2O$(Aesar) were placed in a teflon lined 100ml autoclave in a molar ratio of 1:4 with 75ml of H_2O and heated at 180°C for 2 days. The product containing a mixture of yellow needle-shaped crystals, red crystals, and green powder was washed with distilled water and allowed to air dry. Electron microprobe analysis showed a Bi:Cr ratio of 2:1 for the red crystals and 3:2 for the yellow needles. The red crystals seem to be big enough for a single crystal structure determination but were difficult to isolate as single crystals with a good spot shapes for single crystal structure determination.

The reaction of $NaBiO_3$ with CrO_3 (1:4 ratio) yielded a homogenous yellow powder. This product did not contain crystals large enough for single crystal X-ray diffraction. However, the microprobe analysis showed a Bi:Cr ratio of 3:2, and no Na. The X-ray powder diffraction pattern could be accounted for based on the structure of the yellow needles illustrated in Fig. 4.1.

Thermal gravimetric analysis was conducted using a Netzsch thermal analysis system. A sample of $HBi_3(CrO_4)_2O_3$ was heated to 750°C in air at a rate of 10°/min. Water loss was complete by 400°C. Subsequent oxygen loss led to a plateau from 550° to 750°C. The total weight loss of about 2.5% was considerably less than the 6% expected if the final product contained only Bi^{3+} and Cr^{3+}. The X–ray powder diffraction pattern after dehydration was

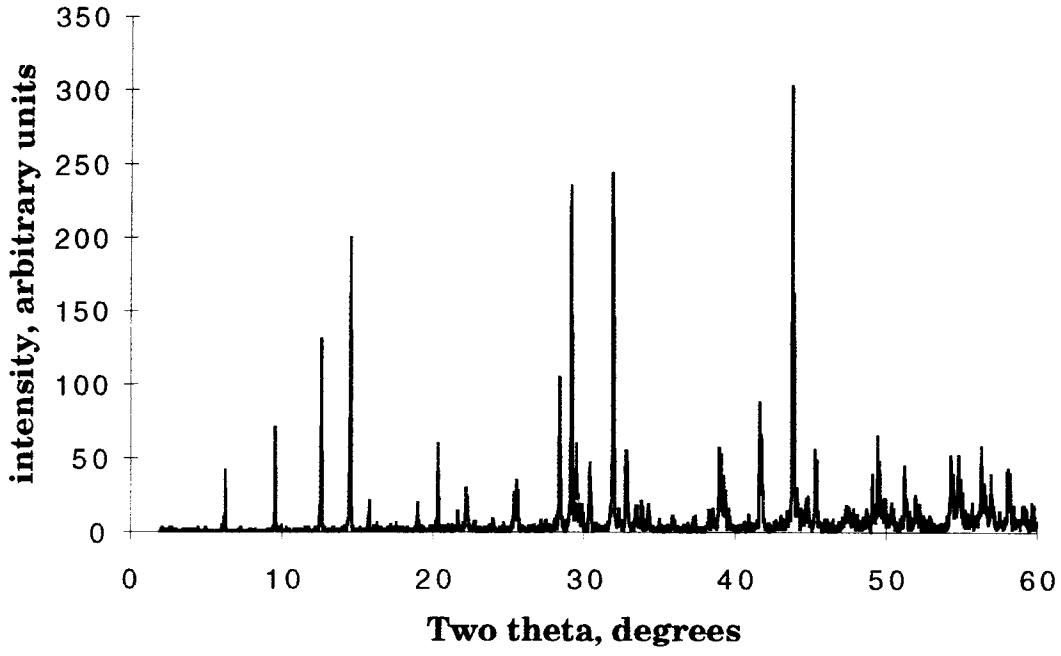

Fig 4.1 Powder pattern of product obtained by the hydrothermal reaction of $NaBiO_3$ with CrO_3

basically that of an amorphous material. X–ray diffraction of the final product showed a strong Bi_2O_3 pattern plus unidentified peaks. However, it should be noted that the known Bi/Cr/O compounds reported (91, 92) contain Cr in an oxidation state higher than +3.

Structure determination

Intensity data on a 0.3mm long yellow crystal were collected using a Rigaku AFC6R diffractometer with graphite monochromated MoK α radiation and the ω -2 θ scan technique. The intensities of three standard reflections, monitored every three hundred reflections throughout the data collection, showed no significant variation. Details of the data collection and refinement are given in the Table 4.1. An empirical absorption correction was made by using the program DIFABS (95). The positions of the bismuth atoms were determined by direct methods using SHELXS (105). A difference fourier analysis gave the positions of the chromium atoms and oxygen atoms. After a least–squares refinement with anisotropic thermal parameters, R = 4.1% and R_W = 4.8%. Charge balance is obtained by adding a hydrogen atom to the formula to give $HBi_3(CrO_4)_2O_3$. The final positional and thermal parameters are given in Tables 4.2 and the anisotropic thermal parameters are shown in Table 4.3. Interatomic distance and angles are given in Table 4.4 and figure 4.2 shows the $HBi_3(CrO_4)_2O_3$ unit cell, and figures 4.3, 4.4, 4.5 show the Bi1, Bi2, Bi3 layers respectively.

Bond-Valence approach

Bond valence calculations were used to locate the possible position of hydrogens in $HBi_3(CrO_4)_2O_3$. According to the bond-valence theory each atoms possesses a valence which is a measure of its bonding power. The valence sum rule that is closely related to Pauling's electrostatic valence rule

Table 4.1

Crystal Data and Intensity Collection for $HBi_3(CrO_4)_2O_3$

Empirical Formula Size (mm^3)	$HBi_3(CrO_4)_2O_3$ 0.3 x 0.1 x 0.1
Formula weight (g/mol)	908
Crystal System	Monoclinic
Space Group	$P2_1/c$, No.14 setting No. 3
a,b,c (Å),ß(°)	5.527(7),12.214(3),14.003(3) 92.95(2)
Volume ($Å^3$)	944.1(3)
Z	4
Diffractometer	Rigaku AFC6R
Radiation	Mo K α (λ = 0.71073Å) Graphite monochromated
Temperature	23°C
Maximum 2 θ (°)	60
Data Collected	0<h<7, 0<k<17,-19<l<19
Scan speed (°/min)	16
Number of data	3144
Number of unique data	1992
Absorption correction	DIFABS
transmission factors	0.52-1.00
refinement method	full-matrix least-squares on |F|
number of parameters	145
R	4.1
Rw	4.8
Goodness of fit	1.4

Table 4.2

Positional and thermal parameters ($Å^2$) for $HBi_3(CrO_4)_2O_3$

Atom	**x**	**y**	**z**	$\mathbf{B_{eq}}^*$
Bi(1)	0.1766(1)	0.37662(5)	0.00425(4)	0.94(2)
Bi(2)	0.2486(1)	0.64154(5)	0.81659(4)	0.89(2)
Bi(3)	0.3222(1)	0.14653(5)	0.56765(5)	1.09(2)
Cr(1)	0.3384(5)	0.3766(2)	0.3925(2)	0.9(1)
Cr(2)	0.1634(5)	0.0923(2)	0.8275(2)	1.0(1)
O(1)	0.898(2)	0.140(1)	0.7937(9)	1.8(5)
O(2)	0.114(2)	0.5438(8)	0.9306(8)	0.9(4)
O(3)	0.814(2)	0.187(1)	0.289(1)	1.9(5)
O(4)	0.021(2)	0.2554(8)	0.1096(8)	0.7(4)
O(5)	0.576(2)	0.074(1)	0.422(1)	1.4(5)
O(6)	0.659(2)	0.918(1)	0.263(1)	1.5(5)
O(7)	0.075(2)	0.978(1)	0.611(1)	1.7((5)
O(8)	0.345(2)	0.784(1)	0.3637(9)	1.4(5)
O(9)	0.041(2)	0.7886(9)	0.524(1)	1.3(5)
O(10)	0.396(2)	0.465(1)	0.124(1)	1.4(5)
O(11)	0.789(3)	0.328(1)	0.912(1)	1.8(5)

$^* B_{eq} = (8\pi^2/3) \sum i \sum j U_{ij} a_i^* a_j^* a_i a_j$

Table 4.3

Anisotropic thermal parameters for $HBi_3(CrO_4)_2O_3$

Atom	U11	U22	U23	U12	U13	U23
Bi(1)	0.0119(3)	0.0124(3)	0.0113(3)	0.0003(2)	0.0020(2)	-0.0004(2)
Bi(2)	0.0130(3)	0.0123(3)	0.0086(3)	-0.0018(2)	0.0000(2)	-0.0009(2)
Bi(3)	0.0128(3)	0.0132(3)	0.0152(3)	-0.0003(2)	0.0001(2)	-0.0010(2)
Cr(1)	0.013(1)	0.014(1)	0.008(1)	0.002(1)	-0.002(1)	0.001(1)
Cr(2)	0.016(1)	0.011(1)	0.009(1)	0.001(1)	-0.002(5)	0.001(1)
O(1)	0.028(7)	0.038(8)	0.003(5)	0.006(6)	-0.002(5)	0.001(5)
O(2)	0.016(6)	0.006(5)	0.011(6)	-0.004(4)	0.006(4)	0.001(4)
O(3)	0.026(7)	0.035(8)	0.012(6)	-0.000(6)	0.001(5)	0.006(6)
O(4)	0.011(5)	0.010(5)	0.006(5)	-0.003(4)	0.003(4)	0.005(4)
O(5)	0.011(6)	0.013(5)	0.028(7)	-0.008(4)	0.009(5)	-0.003(5)
O(6)	0.020(7)	0.022(6)	0.015(6)	-0.002(5)	0.009(5)	0.005(5)
O(7)	0.018(7)	0.026(7)	0.021(7)	0.003(5)	-0.003(5)	-0.008(5)
O(8)	0.009(6)	0.021(7)	0.023(7)	-0.004(5)	0.003(5)	0.003(5)
O(9)	0.023(7)	0.005(5)	0.022(7)	-0.002(5)	0.002(5)	-0.005(5)
O(10)	0.016(6)	0.016(6)	0.020(7)	0.007(5)	0.004(5)	-0.007(5)
O(11)	0.040(8)	0.012(5)	0.015(6)	0.002(5)	-0.010(6)	0.002(5)

Table 4.4

Selected distances (Å) and angles (°) in $HBi_3(CrO_4)_2O_3$

Bi1 O2 2.12(1)	Cr1 O7 1.61(1)
Bi1 O4 2.28(1)	Cr1 O3 1.63(1)
Bi1 O10 2.29(1)	Cr1 O5 1.64(1)
Bi1 O2' 2.30(1)	Cr1 O9 1.70(1)
Bi1 O11 2.52(1)	
Bi1 O4' 2.85(1)	Cr2 O1 1.63(1)
Bi1 O11' 2.89(1)	Cr2 O6 1.64(1)
Bi1 O1 3.25(1)	Cr2 O11 1.66(1)
	Cr2 O10 1.73(1)
Bi2 O4 2.12(1)	
Bi2 O2 2.15(1)	O2 Bi1 O4 72.6(4)
Bi2 O4' 2.24(1)	O4 Bi1 O2 143.9(4)
Bi2 O10 2.47(1)	O2 Bi1 O11 82.9(4)
Bi2 O3 2.58(1)	
Bi2 O3' 2.95(1)	O4 Bi2 O2 102.9(4)
Bi2 O3" 3.42(1)	O4 Bi2 O3 78.8(4)
	O2 Bi2 O3 146.5(4)
Bi3 O8 2.17(1)	
Bi3 O8' 2.20(1)	O8 Bi3 O9 68.0(4)
Bi3 O9 2.31(1)	O8 Bi3 O6 79.6(4)
Bi3 O9' 2.46(1)	O9 Bi3 O6 126.1(4)
Bi3 O6 2.51(1)	
Bi3 O5 2.68(1)	O7 Cr1 O5 107.5(4)
Bi3 O5' 2.76(1)	O3 Cr1 O9 109.1(4)
Bi3 O7 2.90(1)	O1 Cr2 O11 109.6(3)
Bi3 O7' 3.29(1)	O6 Cr2 O10 111.9(3)

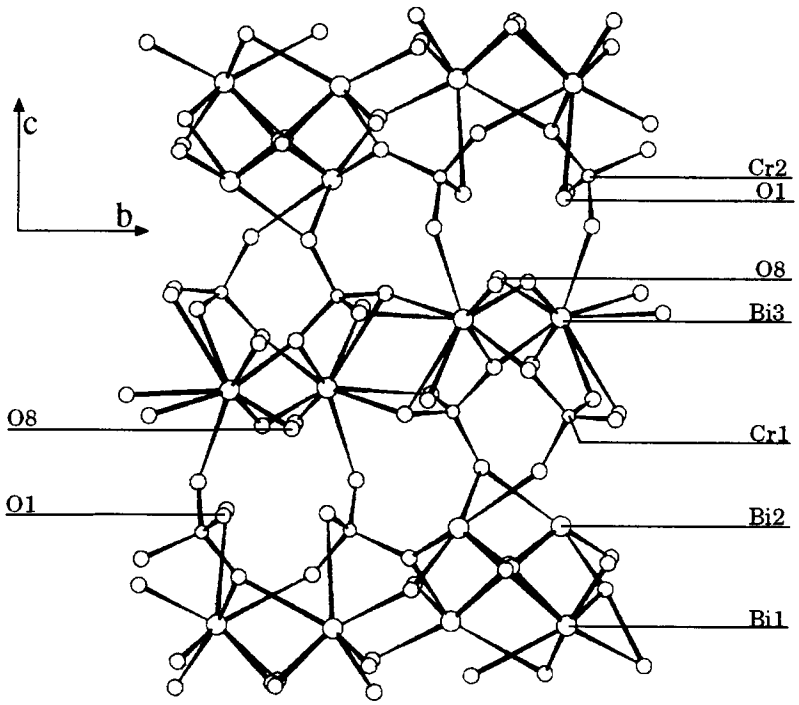

Fig 4.2 $HBi_3(CrO_4)_2O_3$ structure. Small circles are Cr; intermediate circles are O; large circles are Bi. Hydrogen is assumed to be bound to O8 and O1

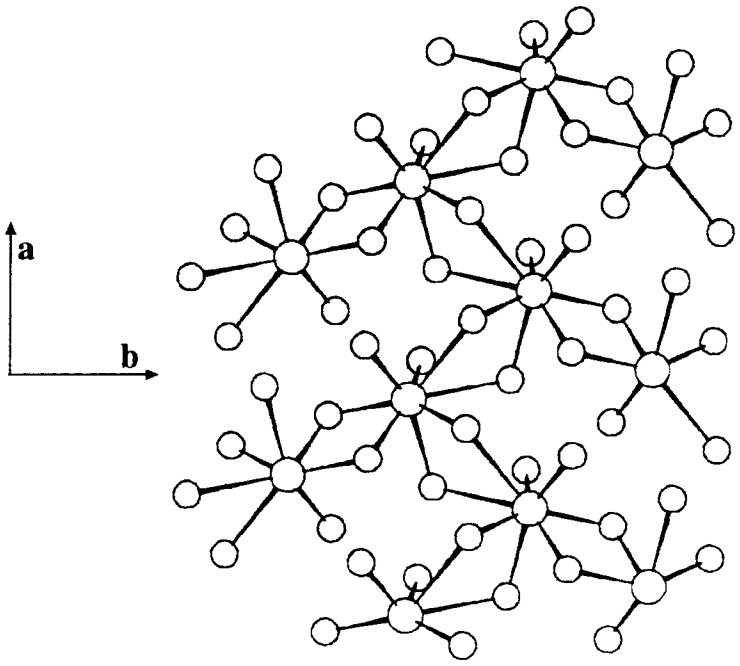

Fig 4.3 The Bi(1) oxide layer. Larger circles are Bi.

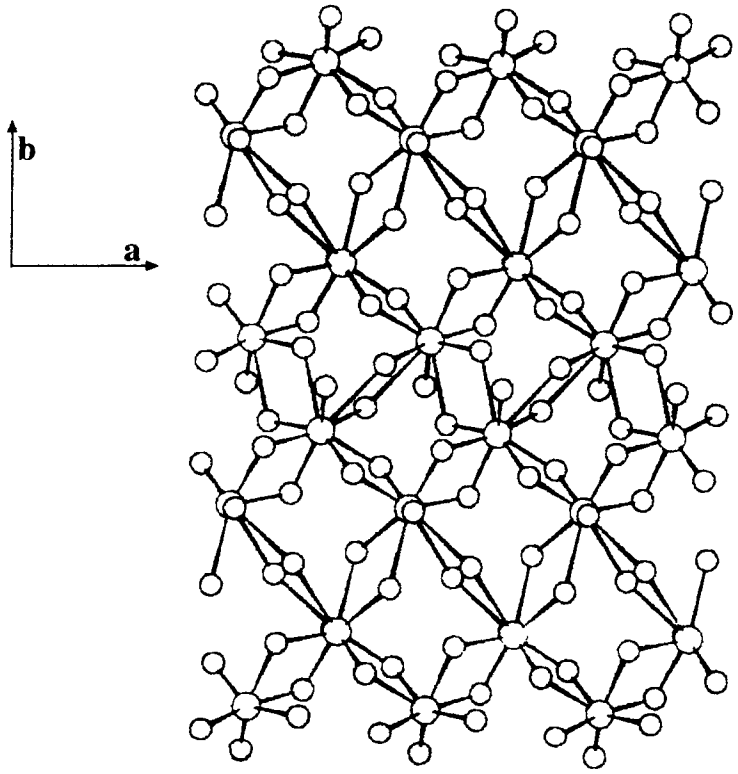

Fig 4.4 The Bi(3) oxide layer. Larger circles are Bi.

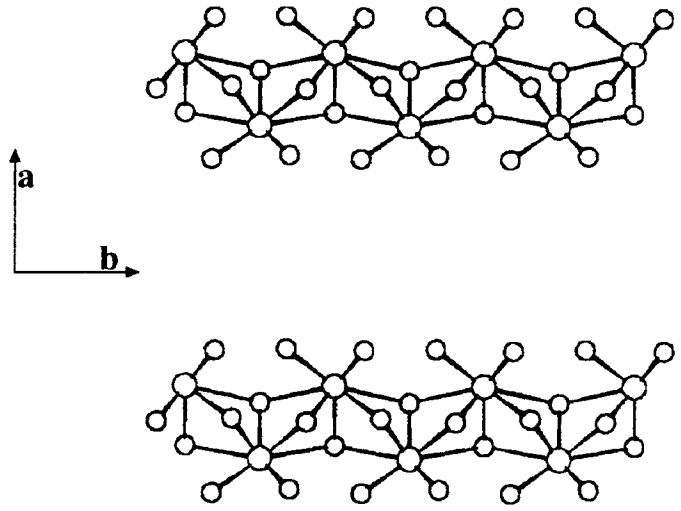

Fig 4.5 The Bi(2) oxide chains. Larger circles are Bi.

states that the sum of bond valences at each atom is equal to the atomic valence.

The bond-valence approach is based on the fact that the bond length is a unique function of bond valence. It is therefore useful to predict and interpret bond lengths in crystals (106, 107). The relationship between bond valence and bond length can be defined by the expression,

$$s = \exp[(R-R_0)/B]$$

Where R is the bond length, and R_0 is the length of a bond of unit valence, B is a fitted constant. If there are discrepancies between experimental and theoretical valences, it may indicate that the structure has not been correctly determined or that it has not been correctly interpreted.

Elements with similar X-ray scattering factors like Si and Al, O and F can be distinguished by the bond valence approach. The valence state of atoms in mixed valent compounds like vanadium oxides are also determined by this method (108). If several atoms are found to have unusually low valences, it may indicate that a molecule of solvent of crystallization has been missed during structure determination. Application of bond-valence method to oxides of Cu in high oxidation states is currently of interest (109,110). Bond valence calculations were used to locate the likely site of hydrogen in $HBi_3(CrO_4)_2O_3$ Both O(1) and O(8) give low valence sums (Table 4.5). These oxygen atoms are 2.68Å apart and are indicated in Fig. 4.1. A hydrogen atom was placed halfway between O(1) and O(8), and the bond valence calculations were repeated. This results in good valence sums (Table 4.5) for both O(1) and O(8). The valence sum for hydrogen is less than expected, and this can be improved by moving hydrogen closer to one of the two oxygens (Table 4.5). Pursing this further did not seem warranted in view of the fact that the valence bond approach is not well suited to compounds containing lone pair cations such as Bi^{3+} (109).

Table 4.5

Results of bond valence calculations for $HBi_3(CrO_4)_2O_3$

Atom	No H	Valences Symmetric[a] H	Asymmetric [b]H
Bi1	3.287	3.287	3.287
Bi2	3.179	3.179	3.179
Bi3	3.396	3.396	3.396
Cr1	5.984	5.984	5.984
Cr2	5.684	5.684	5.684
O1	1.602	1.946	2.314
O2	2.325	2.325	2.325
O3	1.914	1.914	1.914
O4	2.338	2.338	2.338
O5	1.854	1.854	1.854
O6	1.825	1.825	1.825
O7	1.823	1.823	1.823
O8	1.581	1.926	1.748
O9	2.226	2.226	2.226
O10	2.138	2.138	2.138
O11	1.905	1.905	1.905
H		0.688	0.878

a. O(1)-H and O(8)-H = 1.34Å

b. O(1)-H = 1.076Å, O(8)-H = 1.614Å

Discussion

The structure of $HBi_3(CrO_4)_2O_3$ may be described as bismuth oxide layers connected by chromate tetrahedra (Fig. 4.1). The layers are perpendicular to the *c*–axis. The polyhedron of oxygen atoms around Bi(1) is conveniently described using a bismuth coordination number of eight (Fig. 4.5). Six of these oxygen atoms are involved in edge sharing with three like polyhedra. This layer is bound to other bismuth atoms only through chromate tetrahedra. The coordination number of Bi(3) is considered to be nine (Fig. 4.5). Again the polyhedra share edges to form bismuth oxide sheets. However in this case, each polyhedron shares edges with four like polyhedra. A bismuth coordination number of seven is used to describe the polyhedron around Bi(2) (Fig. 4.5) These polyhedra share faces with two like polyhedra to form chains which are parallel to the *a*–axis. However, these chains are tightly bound to the Bi(1) oxide sheet. Thus, we may regard the structure as having Bi(3) oxide sheets and sheets made from both Bi(1) and Bi(2) with oxygen. All three bismuth atoms show evidence of a stereo-active lone pair of electrons. There are short distances on one side, long distances on the opposite side, and intermediate distances around the equator. The chromate tetrahedra are only slightly distorted (Table 4.4).

There are eleven different sites for oxygen. There is two coordination for O(1), O(6) and O(8); three coordination for O(2), O(5), O(7), O(9), O(10)

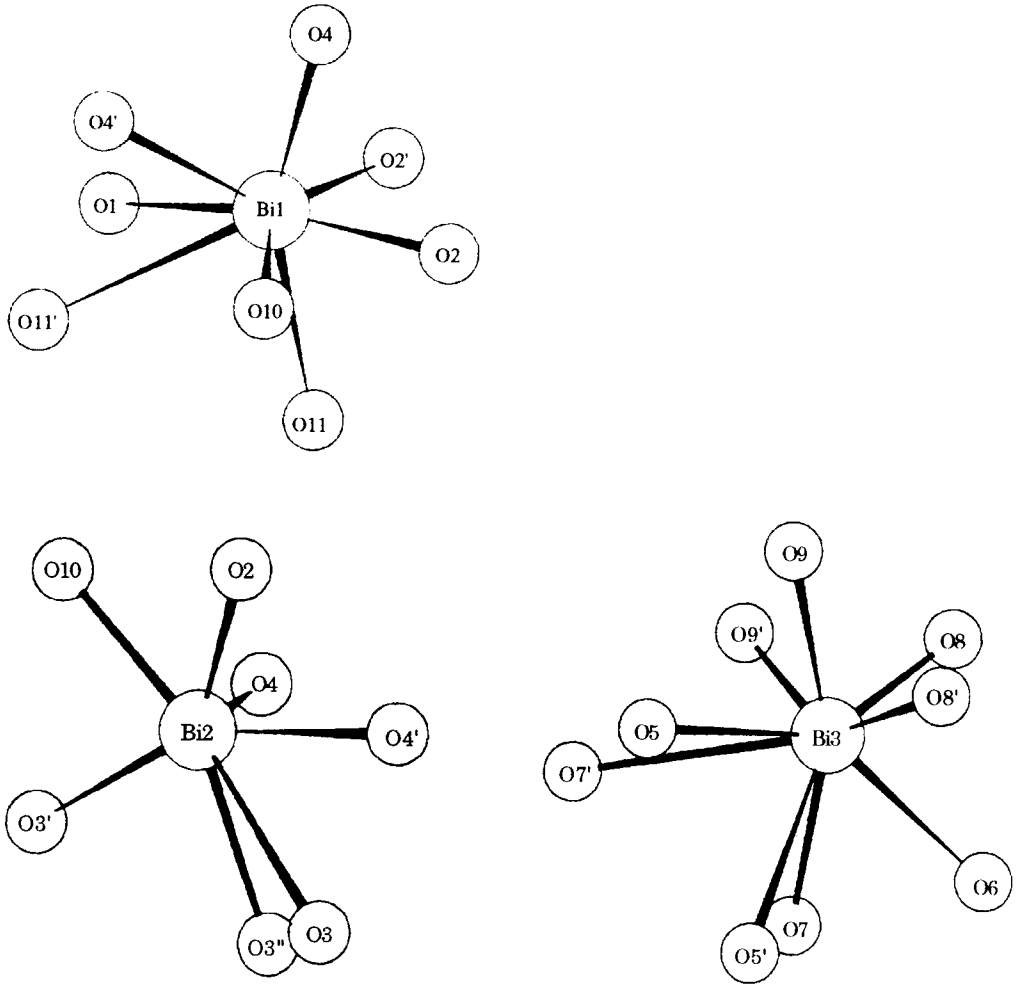

Fig 4.6 Local environment of Bi(1), Bi(2), and Bi(3).

and O(11); and four coordination for O(3) and O(4). Most of the oxygen atoms are coordinated to both chromium and bismuth. However, O(2), O(4) and O(8) are coordinated to bismuth only. Both O(1) and O(8) are considered to be candidates for bonding to hydrogen. Oxygen (1) is bound to one chromium and one bismuth atom whereas O(8) is bound to two bismuth atoms.

Structural Comparison of $HBi_3(CrO_4)_2O_3$ and $Bi(OH)CrO_4$

The structure of the known compound, $Bi(OH)CrO_4$, having one orthorhombic form and one monoclinic form that are closely related is quite different from the new compound made in the course of this study. In both forms of $Bi(OH)CrO_4$, there are layers of $Bi(OH)CrO_4$ perpendicular to the a axis. The bismuth atoms form a puckered, two dimensional network of condensed hexagons, each having two bismuth atoms in the hexagonal array bridged by oxygen atoms or hydroxide groups forming square aggregates of formula $Bi_2O_2^{2+}$ or $Bi_2(OH)_2^{4+}$. The Bi atom has nine-coordination with a polyhedron coordination that can be considered to be a distorted monocapped square antiprism.

The position of the hydrogen atoms were not determined in the two forms of $Bi(OH)CrO_4$. The bond valence approach was applied on these two compounds also. A reasonable position for hydrogen was found for the monoclinic form of this chromate. The results are shown in Table 4.6. In the orthorhombic form, a reasonable position could not be found as shown in Table 4.7

Table 4.6

Bond valence calculations for $Bi(OH)CrO_4$, monoclinic form

Atom	**No H**	**Valences** **Symmetric[a] H**	**Asymmetric[b] H**
Bi	3.227	3.227	3.227
Cr	5.479	5.479	5.479
O1	1.954	1.954	1.954
O2	1.628	1.998	1.809
O3	2.172	2.172	2.172
O4	1.829	1.829	1.829
O5	1.123	1.492	1.876
H		0.739	0.935

a. O2-H = O5-H = 1.318Å

b. O2-H = 1.582Å, O5-H = 1.055Å

Table 4.7

Bond valence calculations for $Bi(OH)CrO_4$, orthorhombic form

Atom	**Valence sum without H**	**Asymmetric H[a]**
Bi	3.271	3.271
Cr	5.535	5.535
O1	2.011	2.011
O2	1.811	1.869
O3	1.603	1.603
O4	2.024	2.024
O5	1.357	1.656
H		0.357

a. O5-H = 1.396Å

Conclusions

The first complete structure determination of a Bi/Cr/O/OH system has been accomplished in solving the crystal structure and using the bond valence approach to locate position of H^+ in the structure. This crystal structure is unique because it does not match any known structure type. The face sharing bismuth - oxygen polyhedra forming a chain is an unusual feature in bismuth oxides.

CHAPTER 5:
STUDIES ON THE $Tl_2Nb_2O_{6+x}$ SYSTEM

Introduction

All the oxide superconductor systems known have mixed valent cations in them, for example Cu^{2+}/Cu^{3+} in cuprates and Bi^{3+}/Bi^{5+} in bismuthates. Additionally, in all these systems there is a insulator-metal transition region (18). The $Tl_2Nb_2O_{6+x}$ system was studied to explore the possibility of superconductivity due to the Tl^{+}/Tl^{3+} mixed valency and an insulator-metal transition with varying oxygen content.

$Tl_2Nb_2O_6$ belongs to the pyrochlore class of compounds. This class of compounds is represented by the general formula $A_2M_2O_6O'$. The A cation is the 8 coordinate cation which is an alkaline earth metal, Tl, rare-earths, Cd, Pb, Sn, etc. The O' oxygen is the special position oxygen. The pyrochlore structure is possible even in the absence of the special oxygen. This class of pyrochlores is called defect pyrochlores. These are especially common with Tl, Pb, Bi, Ag in the A site with lone pair of electrons, since they are polarizable and the A-O, M-O bonds are highly covalent (57).

Fig. 5.1 and 5.2, illustrates the coordination of the two cations and the framework in the pyrochlore structure.

Several systems in the non-copper oxides have been studied to look for metal-insulator transitions and possible superconductivity. Some such examples are pyrochlores like $Tl_2Ru_2O_7$, $Bi_{2-x}Ln_xRu_2O_7$ (111, 112). Despite mixed valency in these compounds superconductivity has not yet been found.

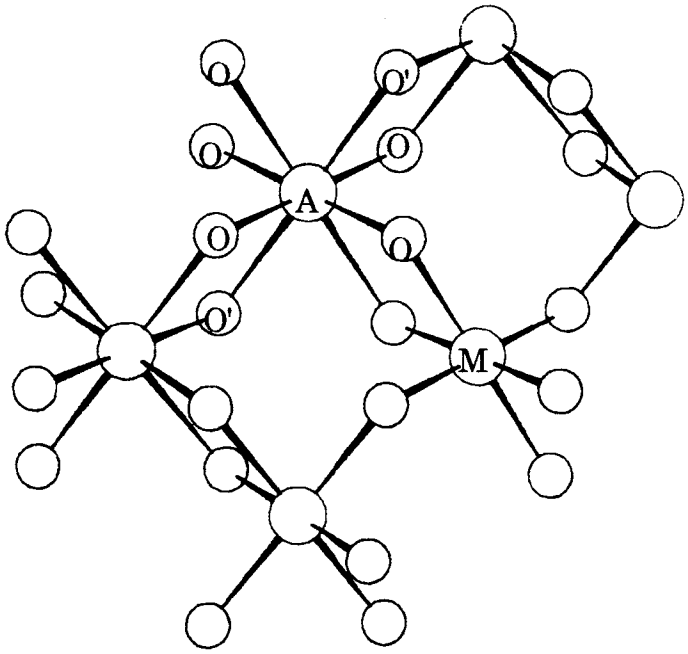

Fig 5.1 Coordination environment of A and M cations in the pyrochlore structure

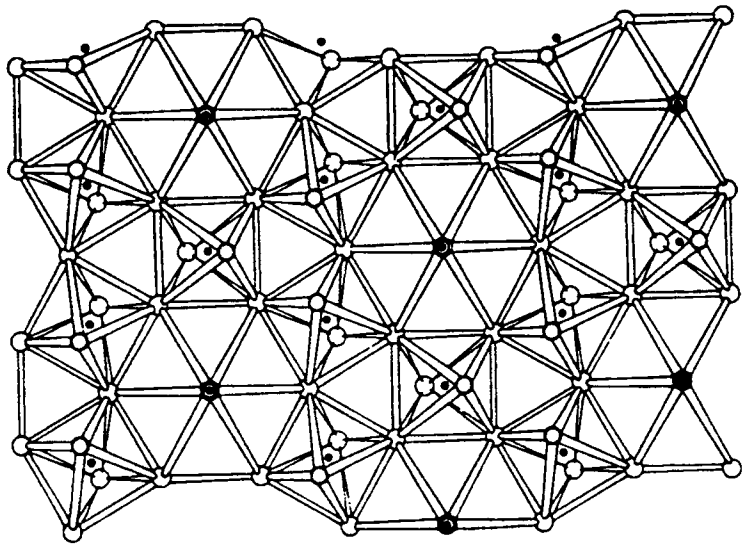

Fig 5.2 Pyrochlore structure based on corner sharing MO_6 octahedra. The two special position oxygens, O' go in and out of the hexagons.

The other oxides known in this ternary system are $TlNb_3O_9$, $Tl_4Nb_6O_{21}$ (113). The pyrochlores $TlBiNb_2O_7$ and $TlPbNb_2O_7$ are also known (114, 115).

In addition to studying the $Tl_2Nb_2O_{6+x}$ system for properties, this system has also been chosen to study for any non-stoichiometry in the A and M sites owing to mixed valency of thallium. In the system, $Sn_2^{2+}M_2^{5+}O_7$, M = Nb,Ta it was observed that both cation and anion vacancies exist in the lattice and Sn^{2+} is partially oxidized to Sn^{4+}, giving rise to the formula, $Sn_{2-x}^{2+}(M_{2-y}^{5+}Sn_y^{4+})O_{7-x-0.5y}$, where x and y vary from 0.48 - 0.10. Thus Sn^{4+} substitues for Nb^{5+} or Ta^{5+} instead of going to the Sn^{2+} site. Mossbauer spectra also confirms the presence of Sn in two different oxidation states (116). Similar results were also observed for the Pb^{2+} containing niobates and tantalates. The general formula can be represented as $Pb_2^{2+(}Pb_x^{4+}M_{2-x}^{5+)}O_{7-0.5x}$ or $Pb_{2-x}^{2+}M_2O_{7-x}$, where B = Nb, Ta or Sb. It was seen that even though stoichiometric $Pb_2M_2O_7$ compounds can be synthesized, they show rhombohedral distortions. (117,118).

Powder neutron diffraction has been used to study the structure of defect pyrochlores (115). There is evidence of oxygen vacancy ordering accompanied by A site cation displacement. $Pb_2Ru_2O_{6.5}$ has been fit in the cubic space group F43m, with the results confirming half occupancy of the defect site, oxygen vacancy ordering and displacement of Pb by 0.04A towards the oxygen vacancy. Similarly, the $PbTlNb_2O_{6.5}$ system has been fit in the tetragonal space group P4m2 using a model that allows ordering of Pb and Tl on the A site with oxygen vacancy ordering. The Rietveld refinement also shows that Pb is displaced slightly away from the oxygen vacancy while Tl is displaced toward this vacancy, resulting in Tl-Tl distances similar to that found in Tl metal.

Experimental

Stoichiometric amounts of Tl_2CO_3 and Nb_2O_5 were ground and allowed to react in an atmosphere of nitrogen at 600°C. A brown powder resulted. This product is $Tl_2Nb_2O_6$.

When stoichiometric amounts of Tl_2CO_3 and Nb_2O_5 were reacted in air at 600°C, a black powder resulted. This product is $Tl_2Nb_2O_{6+x}$.

Another composition was made by the high pressure reaction of Tl_2O_3 with Nb_2O_5 in a sealed gold tube with an external pressure of 3000 atm and temperature of 700°C. This resulted in a black product.

Structural studies

Neutron diffraction studies were done on these samples to get the exact composition. Data were collected at the Brookhaven National Laboratory. The structure was refined from the data collected using GSAS software package (109). Neutron diffraction was done on these samples to get a more accurate oxygen content and to look into the possibility of Tl^{3+} occupying the Nb^{5+} site similar to Pb^{4+} and Sn^{4+} niobates and tantalates.

The structure was refined with initial positional parameters of an ideal pyrochlore type structure. The thallium occupancies refined close to 1.0 in all the compounds indicating that there is very little non-stoichiometry associated with partial occupancy in that site. The lattice parameters of the compounds with higher oxygen content are smaller than those of the compounds with less oxygen. This can be explained based on the fact that the ionic radius of Tl^{3+} is smaller than that of Tl^{1+}. This leads to the contraction in the lattice despite the increase in oxygen content.

In the case of the sample made in nitrogen, the special position oxygen site was almost empty. This is shown in the results of the refinement in table 5.1. In the sample made in air, the special position oxygen occupancy refined to 0.44 giving rise to the formula, $Tl_2Nb_2O_6O'_{0.44}$, while in the sample made under high pressure, the special position oxygen occupany refined close to 0.5 giving the formula, $Tl_2Nb_2O_6O'_{0.5}$. The thermal parameter of the oxygen in special position was high probably due to partial occupancy in that site. In the case of the refinement of the high pressure sample, this was fixed to a reasonable value before refining the occupany of that site.

The results of the Rietveld refinements of these compounds along with their R factors and lattice parameters are given in tables 5.2 and 5.3. Table 5.4 lists the Tl-O, Nb-O distances in these compounds. The observed neutron powder patterns along with the residuals of two of the compositions are illustrated in fig. 5.3 and fig. 5.4.

The thermal parameter for thallium atom was refined anisotropically. It was found that it was highly anisotropic in the compound which was made under nitrogen. In this case, there was essentially no oxygen in the special position. The displacement of thallium atoms in $Tl_2Nb_2O_6$ is along the three fold axis. The partial occupancy observed at O' site might be due to thallium atoms rather than oxygen in that site. In order to establish this, Rietveld analysis was done on the X-ray powder diffraction data, as there is a large difference in the scattering powers of thallium and oxygen. The results of the refinement are given in table 5.5. The thermal parameter for thallium was high as in the neutron data shown in table 5.6. The observed and difference patterns are shown in fig. 5.5. It can be concluded from this data that there is very little oxygen in the special position site and there is no electron density due to thallium in that site.

Table 5.1

Rietveld refinement of $Tl_2Nb_2O_6$, compound made in nitrogen*

a = 10.7134(4) λ = 1.358Å

R_{wp} = 9.08% R_I = 7.11%

Atom	**x**	**y**	**z**	**fraction**
Tl	0.5	0.5	0.5	0.99(1)
Nb	0	0	0	1.0
O	0.3101(1)	0.125	0.125	1.0
O'	0.375	0.375	0.375	0.11(3)

Table 5.2

Rietveld refinement of $Tl_2Nb_2O_6O'_{0.44}$, compound made in air*

a = 10.6365(5) λ = 1.358Å

R_{wp} = 10.65% R_I = 6.85%

Atom	**x**	**y**	**z**	**fraction**
Tl	0.5	0.5	0.5	0.989(8)
Nb	0	0	0	1.0
O	0.3115(1)	0.125	0.125	1.0
O'	0.375	0.375	0.375	0.44(2)

* Also, see appendix

Table 5.3

Rietveld refinement of $Tl_2Nb_2O_6O'_{0.5}$, compound made under high pressure

a = 10.6264(2) λ = 1.8857Å

R_{wp} = 14.6% R_I = 11.3%

Atom	**x**	**y**	**z**	**fraction**
Tl	0.5	0.5	0.5	1.0
Nb	0	0	0	1.0
O	0.3115(1)	0.125	0.125	1.0
O'	0.375	0.375	0.375	0.498(8)

Table 5.4

Compositions and distances in the $Tl_2Nb_2O_{6+x}$ system

Compound	**Nb-O, Å**	**Tl-O, Å**
$(Tl^{I}_{1.89}Tl^{III}_{0.11})Nb_2O_6O'_{0.11}$	1.999	2.778
$(Tl^{I}_{1.89}Tl^{III}_{0.11})Nb_2O_6O'_{0.11}$	1.990	2.748
$(Tl^{I}_{1.89}Tl^{III}_{0.11})Nb_2O_6O'_{0.11}$	1.990	2.743

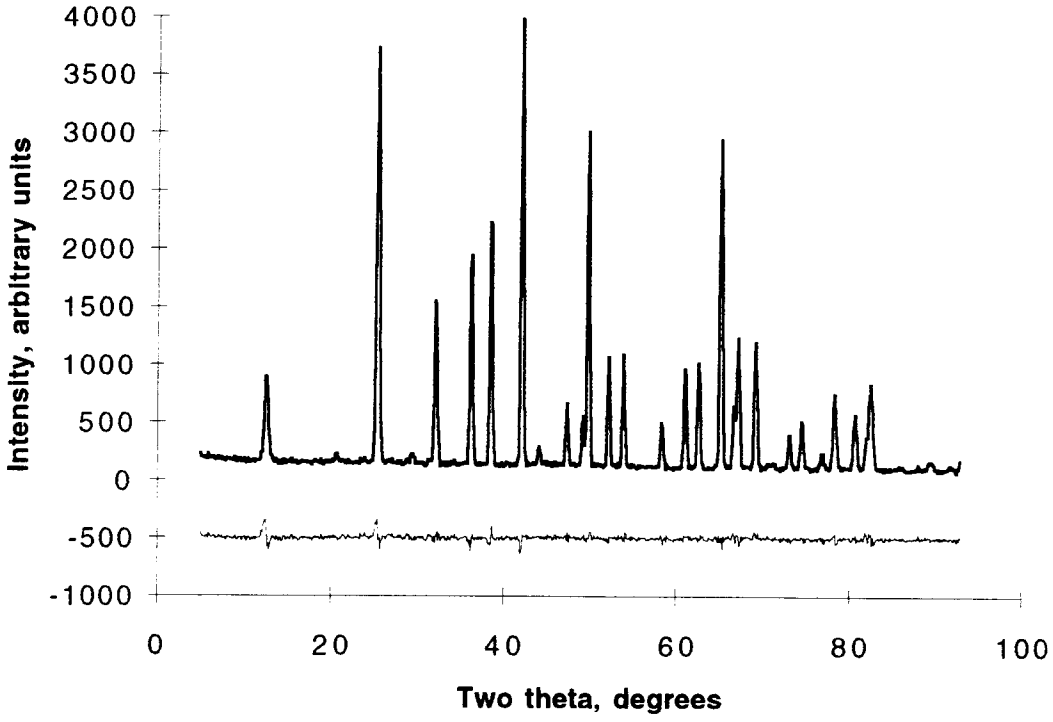

Fig 5.3 Observed and difference pattern in $Tl_2Nb_2O_6$

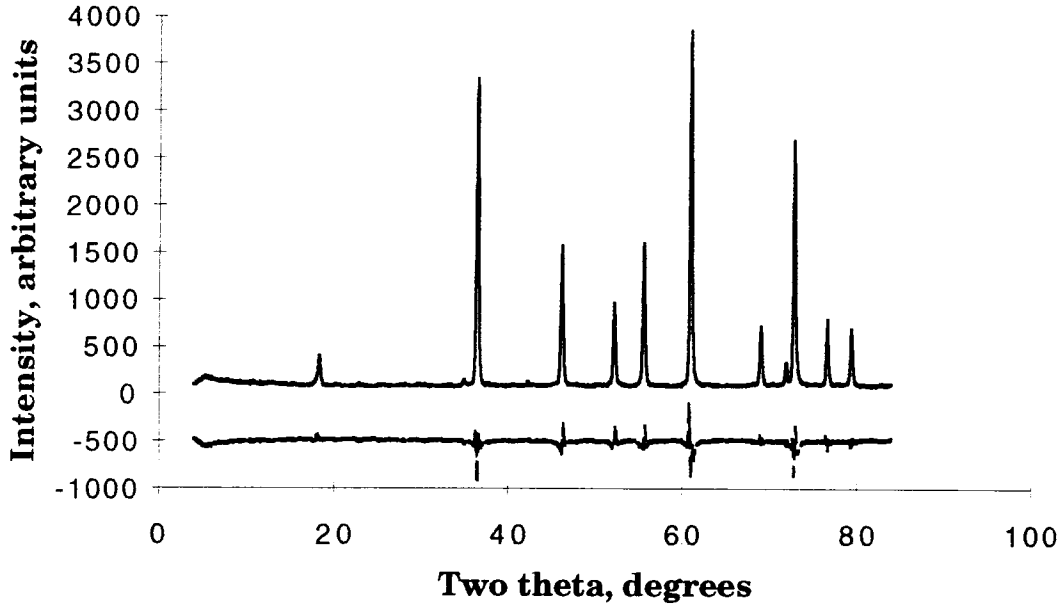

Fig 5.4 Observed and difference pattern in $Tl_2Nb_2O_6O'_{0.5}$

Table 5.5

Positional and thermal parameters for $Tl_2Nb_2O_6$, X-ray Rietveld refinement

R_{wp} = 24.16%
R_I = 9.51%

a = 10.67413(8)

Atom	**Occupancy**	**x**	**y**	**z**	**B**
Tl	1.0	0.5	0.5	0.5	3.3(3)
Nb	1.0	0	0	0	0.1
O(1)	1.0	0.314(6)	0.125	0.125	0.0
O(2)	0.08	0.375	0.375	0.375	0.0

Table 5.6

Thermal parameters for thallium atom from neutron diffraction data

Compound	**B_{eq} Å^2**
$(Tl^{I}_{1.89}Tl^{III}_{0.11})Nb_2O_6O'_{0.11}$	5.40
$(Tl^{I}_{1.89}Tl^{III}_{0.11})Nb_2O_6O'_{0.11}$	2.80
$(Tl^{I}_{1.89}Tl^{III}_{0.11})Nb_2O_6O'_{0.11}$	2.78

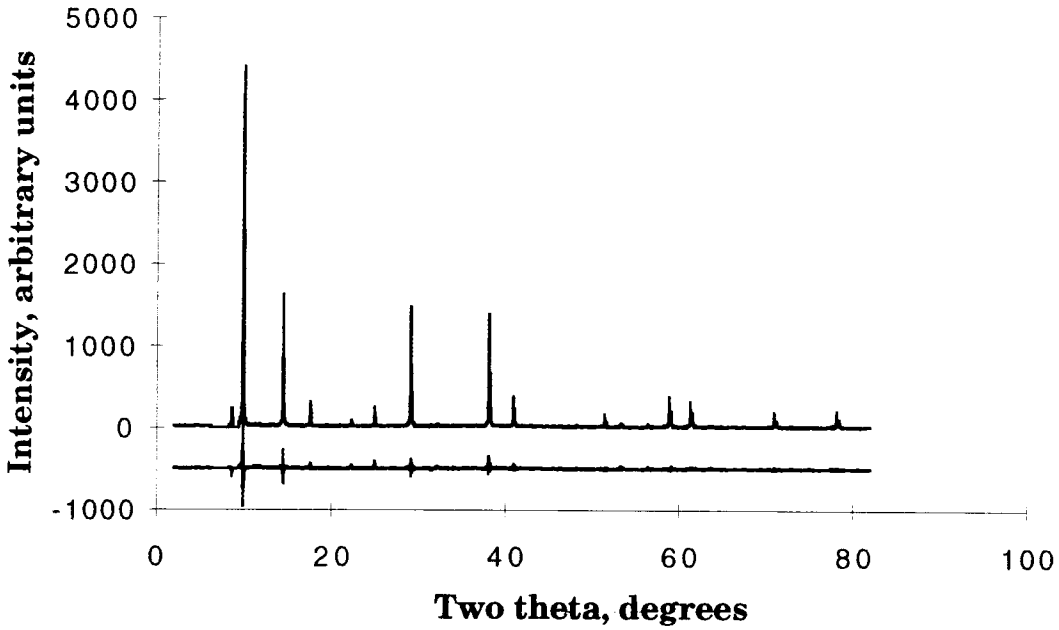

Fig. 5.5 Observed and difference pattern in the X-ray Rietveld refinement of $Tl_2Nb_2O_6$

Conclusions

The oxygen content of compounds in the $Tl_2Nb_2O_{6+x}$ system was determined by using neutron diffraction data. Thallium atom has the highest thermal parameter in the sample with least oxygen and is displaced more towards the oxygen vacancy. No non-stoichiometry was found in the Tl site within experimental error and no mixing of Tl^{III} in the niobium site was observed. The Tl-Tl distances decreased with increasing oxygen content. Insulator to metal transition may be observed if the special position oxygen O' site is fully filled. Therefore this system could be considered as a candidate for superconductivity.

BIBILIOGRAPHY

1. R.J. Cava, B. Batlogg, J.J. Krajeswski, R.Farrow, L.W. Rupp, A.E. White, K. Short, W.F. Peck, T. Kometani, *Nature* **332,** 814 (1988).

2. N.L. Jones, J.B. Parise, R.B. Flippen, A.W. Sleight, *J. Solid State Chem.* **78,** 319, (1989).

3. R.J. Cava, H. Takagi, B. Batlogg, H.W. Zandbergen, J.J. Krajewski, W.F. Peck, R.B. Van Dover, R.J. Felder, T. Siegrist, K. Mizuhashi, J.O. Lee, H. Eisaki, S.A. Carter, S. Uchida, *Nature* **367,** 146 (1994).

4. K. Tanigawa, T.W. Ebbesen, S. Saito, J. Mizuki, J.S. Tsai, Y. Kubo, S. Kuroshima, *Nature* **352,** 222 (1991).

5. A. R. Sweedler, C. Raub and B. T. Matthias, *Phys. Lett.* **15,** 108 (1965).

6. D.C. Johnston, H. Prakash, W.H. Zachariasen and R. Viswanathan, *Mater. Res. Bull.* **8**, 777 (1973).

7.J. K. Burdett and T. Hughbanks, *Inorg. Chem.* **73**, 33 (1988).

8. M.J. Geselbracht, T.J. Richardson and A.M. Stacy, *Nature* **345,** 324 (1990).

9. J.J. Schooley, W.R. Hosler, M.L. Cohen, *Phys.Rev.Lett.* **12,** 474 (1964).

10. Z. Fisk, S.W. Cheong, J.D. Thompson, M.F. Hundley, R.B. Schwarz, G.H. Kwei, J.E. Schirber, *Physica C* **164,** 1681 (1989).

11. D.L. Nelson, M.S. Whittingham and T.F. George (Eds) "*Chemistry of High Temperature Superconductors*", ACS Symp. Series 351, Washington DC (1987).

12. C. Michel, M. Hervieu, M.M. Borel, A. Grandin, F. Deslandes, J. Provost, B. Raveau, *Z. Phys. B* Cond.Matter **68,** 421 (1987).

13. Z.Z. Sheng, A.M. Hermann, *Nature* **332**, 55 (1988).

14. M.A. Subramanian, J. Gopalakrishnan, C.C. Torardi, P.L. Gai, E.D. Boyes, T.R. Askeo, R.B. Flippen, W.E. Farneth, A.W. Sleight, *Physica C* **157,** 124 (1989).

15. H.W. Zandbergen, W.A. Groen, F.C. Mijhoff, G. Van Tendeloo, S. Amelinckx, *Physica C* **156,** 325 (1988).

16. A. Schilling, M. Cantoul, J.D. Guo, H.R. Ott, *Nature* **363,** 56 (1993).

17. D.E. Cox, A.W. Sleight, *Acta Cryst.* **B35,** 1 (1979).

18. A.W. Sleight, *Proceedings of the Robert.A.Welch Foundation Conference on Chemical Research XXXII VALENCY.*

19. A.W. Sleight, J.L. Gillson, P.E. Bierstedt, *Solid State Commun.* **17,** 27 (1975).

20. D. Tseng, E. Ruckenstein, *Mater. Lett.* **8,** 69 (1989).

21. M.A. Subramanian, *J. Solid State Chem.* **111,**134 (1994).

22. Q. W. Chen, Y.T. Qian, Z.Y. Chen, K.B. Tang, G.E. Zhou, Y.H. Zhang, *Physica C* **224,** 228 (1994).

23. M.L. Norton, *Mat. Res. Bull.* **24,** 1391 (1989).

24. G.L. Roberts, S.M. Kauzlarich *unpublished results*

25. M.B. Robin, K. Andres, T.H. Geballe, N.A. Kuebler, D.B. Mcwhan, *Phys. Rev. Lett.* **17,** 917 (1966).

26. J.L. Andrieux, *Rev. Met.* **45,** 49 (1948).

27. A. Wold, D. Bellavance, *Preparative Methods in Solid State Chemistry;* P. Hagenmuller, Ed.; Academic Press: New York, 1972, p 279.

28. L.N. Demianets, A.N. Lobachev, *Current Topics in Materials Science;* E. Kaldis, Ed.; North-Holland Publishing Co. : Amsterdam (1981).

29. R.K. Grasselli, J.D. Burrington, J.F. Bradzil *Faraday Discuss. Chem.Soc.* **72,** 203 (1981).

30. T. Chen, G.S. Smith, *J. Solid State Chem.* **13,** 288 (1975).

31. T. Lu, B.C.H. Steele, *Solid State Ionics* **21,** 339 (1986).

32. P. Nielson, S. Ivasa, *Appl. Opt.* **11,** 2760 (1972).

33. F.P. Strohkendl, R.W. Helwarth, *J. Appl. Phys.* **62,** 2455 (1987).

34. M.G. Jani, L.E. Halliburton, *J. Appl. Phys.* **64,** 2022 (1988).

35. S.C. Abrahams, P.B. Jamieson, J.L. Bernstein, *J. Chem. Phys.* **47,** 4034 (1967).

36. J. Huang, A.W. Sleight, *U.S. Patent* No. 5, 202, 891, April 13 1993.

37. N. Kumada, N. Kinomura, S. Kodialam, A.W. Sleight, *Mater. Res. Bull.*

29, 497 (1994).

38. F. Hullinger, *Structural Chemistry of Layer-type phases*, P. 258, D. Reidel Publishing Co., Boston (1976).

39. W. Zhou, R.H. Jones, J.M. Thomas and D. Bieber, *Chem. Mater.* **2,** 216 (1990)

40. Feigelson, R. S. In *Solid State Chemistry: A Contemporary Overview*; Holt, S.L., Milstein, J.B. Robbins, M., Eds.; American Chemical Society: Washington, DC, 1980.

41. M.L. Norton, H.Y. Tang, *Chem. Mater.* **3,** 431(1991).

42.R. Bezzenberger, R. Schollhorn, *Eur. J. Solid State Chem.* **30,** 435 (1993).

43. C. Chaillout, J. Durr, C. Escribe-Filippini, T. Fournier, J. Marcus, M. Marezio, *J. Solid State Chem* **93,** 63 (1991).

44. N. Szabo, G. Argay, *Acta Cryst*. **19,** 180 (1965).

45. B. Standke, M. Jansen, *Angew. Chem.,Int. Ed. Engl.*, **24,** 118 (1985). 46.

M. Jansen, Uta Bilow, *J. Alloys Compounds*, **183,** 45 (1992).

47. R. Hubenthal, R. Hoppe, *Acta. Chem. Scand* **45,** 805 (1991).

48. J. Pannetier, D. Tranqui, A.W. Sleight, *Mater. Res. Bull*. **28,** 989 (1993).

49. V. A. Carlson, A.M. Stacy *J.Solid State Chem*. **96,** 332 (1992).

50. S.Uma, J. Gopalakrishnan, *J.Solid state Chem*, **105,** 595 (1993).

51. A. prokopcikas, G. Rozovskis, *Lietuvos TSR Mokslu Akad.Darbai*. Ser.B **3,** 181 (1961).

52. R.N. Bhattacharya, R. Noufi, L.L. Roybal, R.K. Ahrenkiel, *J. Electrochem. Soc*. **136,** 1643 (1991).

53. P. Slezak, A. Wieckowski, *J. Electrochem. Soc*. **138,** 1038 (1991).

54. T.Wade, R.M. Crooks, E.G. Garza, D.M. Smith, J.O. Willis, J.Y. Coulter, *Chem. Mater.* **6,** 87 (1994).

55. T. Wade, J. Park, E.G. Garza, C.B. Ross, D.M. Smith, R.M. Crooks, *J. Am. Chem. Soc*. **114,**9457 (1992).

56. L.F. Mattheiss, E.M. Gyorgy,D. W. Johnson, *Phys. Rev*. **B37,** 3745 (1988).

57. M.A. Subramanian, G. Aravamudan, G.V. Subba Rao,

Prog. Solid State Chem. **15,** 55 (1983).

58. N. Kumada N. Kinomura, *Mater. Res. Bull.* **28,** 849 (1993).

59. Daniel M. Giaquinta and Hans-Conrad Zur Loye, *Chem. Mater.* **6,** 365 (1994)

60. J.B. Goodenough, J.A. Kafalas, *J. Solid State Chem.* **6,** 493 (1973).

61. H.Y.P. Hong, J.A. Kafalas, J.B. Goodenough *J. Solid State Chem.* **9,** 345, (1974).

62. R. Scholder, H. Stobbe, *Z. Anorg. Allg.Chem.* **247,** 392 (1941).

63. J. Trehoux, F. Abraham, D. Thomas, *Mater. Res. Bull.* **17,** 1235 (1982).

64. J. Trehoux, F. Abraham D. Thomas, *J. Solid State Chem.* **21,** 203 (1977).

65. J. Trehoux, F. Abraham, D. Thomas, *Mater. Res. Bull.* **17,** 309 (1982).

66. S. Kodialam, V.C. Korthuis, R.D. Hoffmann, A.W. Sleight, *Mater. Res. Bull.* **27,** 1379 (1992).

67. G.A. Mabbott, *J. Chem. Ed.* **60**, 697 (1983).

68. G.L. Roberts, S.M. Kauzlarich, R.S. Glass, J.C. Estill *Chem. Mater.* **5,**1645 (1993).

69. C.R. Peters, M. Bettman, J.W. Moore, M.D. Glick, *Acta.Cryst.* Sect. **B27,** 1826 (1971).

70. T.N. Nguyen, D.M. Giaquinta, W.M. Davis Hans-Conrad zur Loye, *Chem. Mater.* **5,** 1273 (1993).

71. J.M. Longo, A.W. Sleight, *Inorg. Chem.* **7,** 108 (1968).

72. F. Abraham, D. Thomas, G. Nowogrocki, *Bull. Soc. fr. Mineral. Cristallogr.* **98,** 25 (1975).

73. A. W. Sleight, R.J. Bouchard, *Inorg. Chem.* **12**, 2314 (1973).

74. M. Jansen, *Z. Naturforsch.* **32b,** 1340 (1977).

75. J. Zemann, Anz. *Osterr. Akad. Wiss.* **85,** 85 (1948).

76. R. Marchand, L. Brohan, M. Tournaux, *Mater. Res. Bull.* **15,** 1129 (1980).

77. Q. Le Thi, J.P. Besse, R. Chevalier, *Mater. Chem. Phy.* **15,** 167 (1986).

78. O.M. Hamedi, J.P. Besse, G. Baud R.Chevalier, *Mater. Res. Bull.* **19,** 487, (1984).

79. F. Honnart, J.C. Boivin, D. Thomas, K.J. De Vries, *Solid State Ionics* **9&10,** 921 (1983).

80. N. Kinomura, M. Hosoda, N. Kumada, H. Kojima, *J.Ceram.Soc.Japan* **101,** 966 (1993).

81. N. Kumada, M. Hosada and N. Kinomura, *J. Solid State Chem* **106,** 476 (1993)

82. A. Jager and D. Kolar *J. Solid State Chem.* **53,** 35 (1984).

83. T. Graia, P. Conflant, G. Nowogrocki, J.C. Boivin and D. Thomas, *J. Solid State Chem*, **63,** 160, (1986).

84. M.A. Subramanian, *Mater. Res. Bull.* **25,** 107 (1990).

85. F. Izumi, *Rigaku J.* **6,** 10 (1989).

86. W.E. Klee and G. Weitz, *J.Inorg.Nucl.chem.* **31,** 2367 (1969).

87. A.W. Sleight, *Inorg. Chem* **8,** 1807 (1969).

88. M.A. Subramanian, A.K. Ganguli, A.W. Sleight, *Mater. Res. Bull.* **27,** 799 (1992).

89. B. Begemann, M. Jansen *J. Less-common metals* **156,** 123 (1989).

90. N. Kumada, N.Kinomura, P.M. Woodward, A.W. Sleight *in preparation for publication.*

91. E.M. Levin, R.S. Roth, *J. Res. Nat. Bur. Stand.* **68A,** 197 (1964).

92. K. Masuno, *J. Chem. Soc. Japan*, **90,** 1122 (1969).

93. F. Sugawara, S. Iida, *J. Phys. Soc. Japan*, **20,** 1529 (1965).

94. F. Sugawara, S. Iida, *J. Phys. Soc. Japan*, **25,** 1553 (1968).

95. B. Aurivillius, I. Jonsson, *Arkiv. Kemi.* **19,** 271 (1962).

96. B. Aurivillius, A. Lowenhielm, *Acta. Chem. Scand.* **18,** 1937 (1964).

97. H. Harawalt et al. *Anal. Chem.* **10,** 475 (1938).

98. L.B. Sillen, *Arkiv. fr. Kemi. Minera. Geol.* **12A,** 1 (1937).

99. R.W. Wolfe, R.E. Newnham, *Solid State Commun.* **7,** 1797 (1969).

100. R.E. Newnham, R.W. Wolfe, J.F. Dorrian, *Mater. Res. Bull.* **6,** 1029 (1971).

101. J.M. Longo, R.M. Raccah, J.A. Kafalas, J.W. Pierce, *NBS Special Publ. (U.S.)*, No.**364,** 219 (1972).

102. A. Ramanan, G.N. Subbanna, J. Gopalakrishnan, C.N.R. Rao, *Rev.Chim.Miner.* **20,** 576 (1983).

103. I. Bueno, C.Parada, E. Gutierrez Puebla, A. Monge, C. Ruiz Valero *J. Solid State Chem*. **78,** 78 (1989).

104. S. Habekost, A. Norlund Christensen, R. G. Hazell *Acta Chem. Scand*. **45**, 6 (1991).

105. Molecular Structure Corporation, "*Texsan*", The Woodlands, TX, 1989.

106. I.D. Brown and D. Altermatt, *Acta cryst.* **B41,** 244 (1985).

107. N.E. Brese and M.O' Keeffe, *Acta Cryst*. **B47,** 192 (1991).

108." *Structure and Bonding in Crystals*", Volume II Edited by M.O' Keeffe, Alexandra Navrotsky, Academic Press, 1981.

109. I.D. Brown, *J. Solid State Chem.* **82,** 122 (1989).

110. M. O'Keeffe, S. Hansen *J. Am. Chem. Soc.* **110,** 1506, (1988).

111. "*Valence Instabilities and related narrow-band phenomena*", Edited by R.D. Parks, Plenum Publishing Corporation, p545-549 (1977).

112. T. Yamamoto, R. Kanno, Y. Takeda, O. Yamamoto, Y. Kawamoto, M. Takano, *J.Solid State Chem.*. **109**, 372 (1994).

113. S.S. Plotkin, V.E. Plyushchev, L.S. Moiseeva, *Neorgan. Mater.* **7**, 2041 (1971).

114. A. Ramanan, J. Gopalakrishnan, C.N.R. Rao, *J.Solid State Chem.* **60,** 376 (1985).

115. R.A. Beyerlein, H.S. Horowitz, J.M. Longo, M.E. Leonowicz, J.D. Jorgensen, F.J. Rotella, *J.Solid State Chem.* **51,** 253 (1984).

116. T. Birchall, A.W. Sleight, *J. Solid State Chem*. **13,** 118, (1975).

117. G. Burchard, W. Rudorff, *Z. anorg. allg. chem*, **344,** 23 (1966).

118. E.C. Subbarao, *J.Am. Ceram. Soc.* **44,** 92 (1961).

119. *'GSAS", General Structure Analysis System*, A.C. Larson, R.B. Von Dreele, Los Alamos National Laboratory (1990).

APPENDIX 1

Rietveld Considerations

$M = \sum w (I_o - I_c)^2$

The residuals are,

$$R_I = \frac{\sum |I_o - I_c|}{\sum I_o}$$

$$R_{wp} = \frac{(M)^{1/2}}{(\sum w I_o^2)^{1/2}}$$

$$R_F = \frac{\sum | (I_o)^{1/2} - (I_c)^{1/2} |}{\sum (I_o)^{1/2}}$$

The variance of the peak, σ^2 varies with 2θ according to,

$$\sigma^2 = U\tan 2\theta + V\tan\theta + W + F_2/\tan^4\theta$$

The neutron powder diffraction data collected on the $Tl_2Nb_2O_{6+x}$ system for the compounds synthesized in air and nitrogen were low resolution data and the data collected on the sample made under high pressure was high resolution data. The profile parameters, U, V, W for these refinements were,

Sample	**U**	**V**	**W**
$Tl_2Nb_2O_6$	1.056E+03	-8.457E+02	3.258E+02
$Tl_2Nb_2O_6O'_{0.44}$	1.495E+03	-1.220E+03	4.346E+02
$Tl_2Nb_2O_6O'_{0.5}$	1.124E+02	-8.401E+01	1.822E+02